

# Accepted Manuscript

2,4-Disubstituted quinazolines targeting breast cancer cells via EGFR-PI3K

Er-dong Li, Qiao Lin, Ya-qi Meng, Lu-ye Zhang, Pan-pan Song, Na Li, Jing-chao Xin, Peng Yang, Chong-nan Bao, Dan-qing Zhang, Yang Zhang, Ji-kuan Wang, Qiu-rong Zhang, Hong-min Liu



PII: S0223-5234(19)30248-X

DOI: <https://doi.org/10.1016/j.ejmech.2019.03.030>

Reference: EJMECH 11200

To appear in: *European Journal of Medicinal Chemistry*

Received Date: 24 January 2019

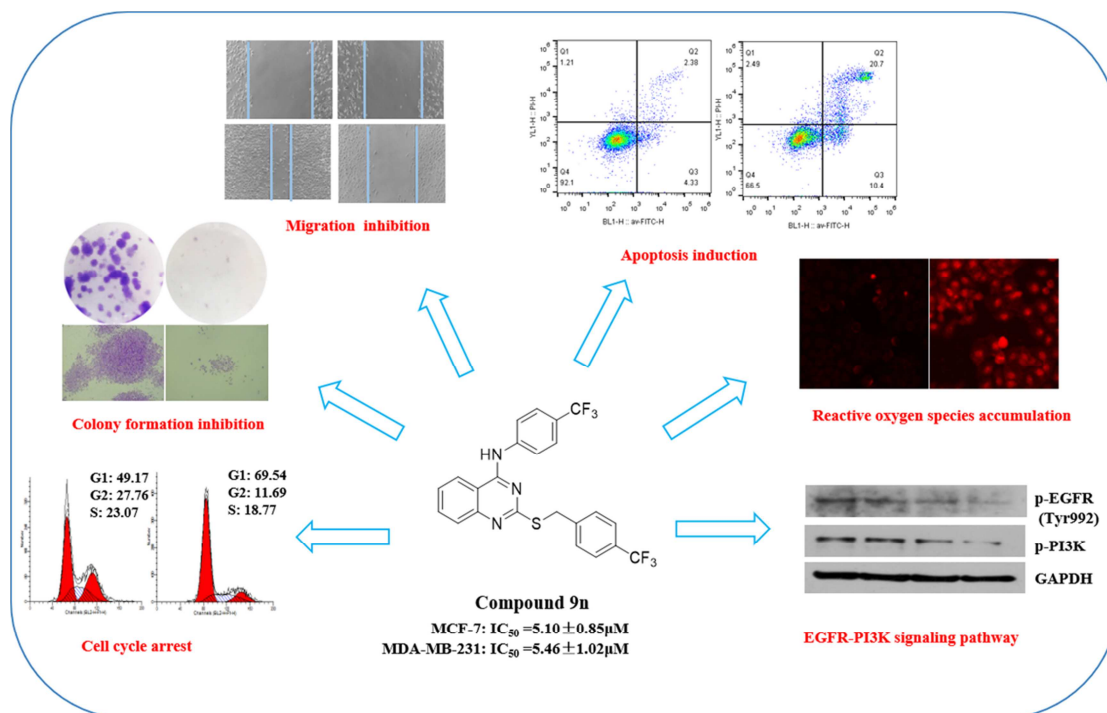
Revised Date: 12 March 2019

Accepted Date: 13 March 2019

Please cite this article as: E.-d. Li, Q. Lin, Y.-q. Meng, L.-y. Zhang, P.-p. Song, N. Li, J.-c. Xin, P. Yang, C.-n. Bao, D.-q. Zhang, Y. Zhang, J.-k. Wang, Q.-r. Zhang, H.-m. Liu, 2,4-Disubstituted quinazolines targeting breast cancer cells via EGFR-PI3K, *European Journal of Medicinal Chemistry* (2019), doi: <https://doi.org/10.1016/j.ejmech.2019.03.030>.

This is a PDF file of an unedited manuscript that has been accepted for publication. As a service to our customers we are providing this early version of the manuscript. The manuscript will undergo copyediting, typesetting, and review of the resulting proof before it is published in its final form. Please note that during the production process errors may be discovered which could affect the content, and all legal disclaimers that apply to the journal pertain.

## Graphical abstract



## 2,4-Disubstituted quinazolines targeting breast cancer cells via EGFR-PI3K

Er-dong Li<sup>a,b</sup>, Qiao Lin<sup>a,b</sup>, Ya-qi Meng<sup>a,b</sup>, Lu-ye Zhang<sup>a,b</sup>, Pan-pan Song<sup>a,b</sup>, Na Li<sup>a,b</sup>, Jing-chao Xin<sup>a,b</sup>,  
Peng Yang<sup>a,b</sup>, Chong-nan Bao<sup>a,b</sup>, Dan-qing Zhang<sup>a,b</sup>, Yang Zhang<sup>a,b</sup>, Ji-kuan Wang<sup>a,b</sup>, Qiu-rong  
Zhang<sup>\*.a,b</sup>, Hong-min Liu<sup>\*.a,b</sup>

<sup>a</sup> School of Pharmaceutical Sciences, Zhengzhou University, Zhengzhou 450001, PR China

<sup>b</sup> Collaborative Innovation Center of New Drug Research and Safety Evaluation, Zhengzhou 450001,  
PR China

\*Corresponding Authors: Qiu-rong Zhang, Ph.D & Hong-Min Liu, Ph.D

Zhengzhou University, Zhengzhou, 450001, PR China

E-mail: zqr409@yeah.net (Qiu-rong Zhang) & liuhm@zzu.edu.cn (Hong-min Liu)

**Abstract**

A series of novel 2,4-disubstituted quinazolines were synthesized and evaluated for their anti-tumor activity against five human cancer cells (MDA-MB-231, MCF-7, PC-3, HGC-27 and MGC-803) using MTT assay. Among them, compound **9n** showed the most potent cytotoxicity against breast cancer cells. Compound **9n** also significantly inhibited the colony formation and migration of MDA-MB-231 and MCF-7 cells. Meanwhile, compound **9n** induced cell cycle arrest at G1 phase and cell apoptosis, as well as increased accumulation of intracellular ROS. Furthermore, compound **9n** exerted anti-tumor effects in vitro via decreasing the expression of anti-apoptotic protein Bcl-2 and increasing the pro-apoptotic protein Bax and p53. Mechanistically, compound **9n** markedly decreased p-EGFR and p-PI3K expression, which revealed that compound **9n** targeted breast cancer cells via interfering with EGFR-PI3K signaling pathway. Molecular docking suggested that compound **9n** could indeed bind into the active pocket of EGFR. All the findings suggest that compound **9n** might be a valuable lead compound for anti-tumor agents targeting breast cancer cells.

**Key words: Quinazoline, Breast cancer, EGFR-PI3K**

## 1. Introduction

The epidermal growth factor receptor (EGFR) plays an important role in cellular functions [1-4], and it is often over-expressed and uncontrolled in a variety of human tumor cells [5]. PI3K especially as a downstream protein of EGFR signaling pathway is dysregulated in breast cancer, non-small-cell lung cancer, colorectal cancer and prostate cancer [6-10]. The EGFR-PI3K signaling pathway not only affects the proliferation, differentiation, invasion and metastasis of tumor cells, but also plays a key role in the treatment of tumors [11-14]. Therefore, targeting EGFR-PI3K pathway is one of the effective ways to treat tumors.

Quinazoline derivatives are valued for their diverse pharmacological properties such as anti-tumor, antimalarial, antibacterial, anti-inflammatory, anti-convulsant and anti-diabetic activities [15-19]. In recent years, many quinazoline-based compounds have been approved for clinical use by US Food and Drug Administration (FDA) including Gefitinib, Erlotinib and Lapatinib [20-24] (Fig. 1). Based on the study of the structure-activity relationship of quinazoline derivatives [25], the 4-aminoquinazoline was selected as the scaffold to study.

Meanwhile, it has been reported that compound **1**, compound **2**, and compound **3** have superior anti-tumor effects on tumor cells, and all of them contain 4-trifluoromethylbenzyloxy group [26-28] (Fig. 1). Inspired by the results of the above studies, 4-trifluoromethylbenzyl was linked to the sulfhydryl group at position 2 of the quinazoline by the principle of molecular hybridization. Then, we synthesized a series of 2,4-disubstituted quinazolines and evaluated their bioactivity in vitro. Finally, western blotting and molecular docking were performed to explore the possible mechanism of activity of the compounds on breast cancer cells.

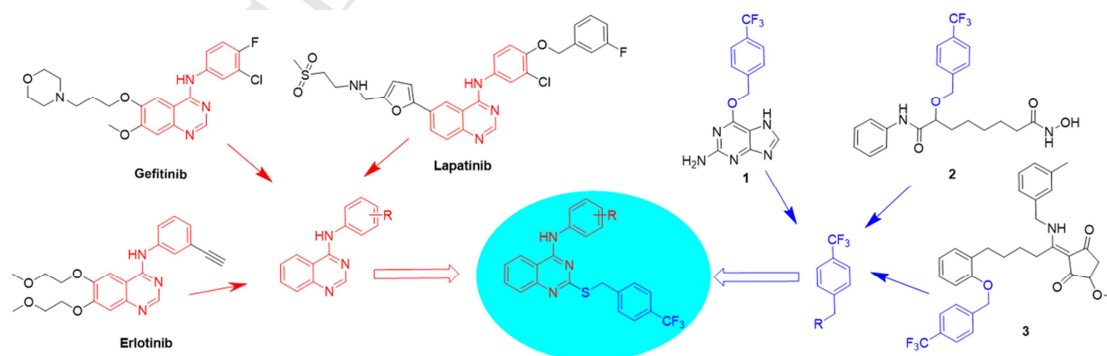
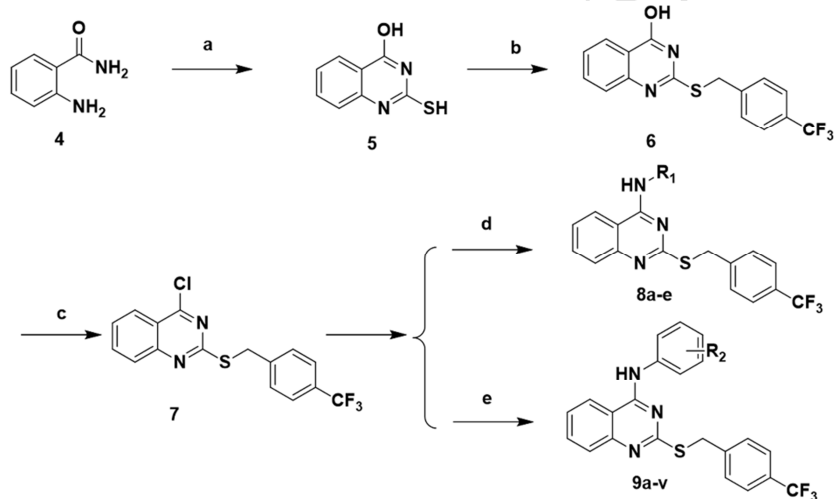


**Fig.1** Anti-tumor agents and design of 2,4-disubstituted quinazolines.

## 2. Results and discussion

### 2.1. Chemistry

The synthetic strategy to prepare the target compounds is depicted in Scheme 1. Compound **5** was prepared by the reaction of 2-anthranilamide (compound **4**) with carbon disulfide in the presence of KOH in ethanol for 36h. Then, compound **6** was acquired from the reaction of compound **5** with 4-trifluoromethylbenzyl chloride under basic condition in the mixture of H<sub>2</sub>O and 1,4-dioxane for 4h in 84.5% yield, that was further reacted with phosphorus oxychloride at 65 °C for 1h to get compound **7** in 83% yield. Next, the compound **7** was reacted with different amines to obtain compound **8a-e** and **9a-v** in 54.7-84.2% yield. Finally, all the target compounds were fully characterized by <sup>1</sup>H NMR, <sup>13</sup>C NMR and HRMS.



**Scheme 1.** Reagents and conditions: (a) CS<sub>2</sub>, KOH, EtOH, reflux, 36h; (b) 4-trifluoromethylbenzyl chloride, KOH, H<sub>2</sub>O, 1,4-dioxane, 90 °C, 4h, HCl; (c) POCl<sub>3</sub>, 65 °C, 1h; (d) Alkyl amines, Isopropanol, reflux, 6h. (e) Aromatic amines, DMF, 90 °C, 4h.

### 2.2. Evaluation of biological activity

#### 2.2.1 Antiproliferative activity

In order to explore the anti-tumor effect of the target compounds, compounds **8a-e** and **9a-v** were evaluated against five human cancer cells, including MDA-MB-231 (Human breast cancer cell line), MCF-7 (Human breast cancer cell line), PC-3 (Human prostate cancer cell line), HGC-27 (Human gastric carcinoma cell line) and MGC-803 (Human gastric carcinoma cell line) using MTT assay. Gefitinib was employed as the positive control. The results are shown in Table 1.

**Table 1** Cytotoxicity of 2,4-disubstituted quinazolines **8a-e** and **9a-v** against five human cancer cells.

Compound	R	IC <sub>50</sub> ( $\mu$ M) <sup>a</sup>				
		MDA-MB-231	MCF-7	PC-3	HGC-27	MGC-803
<b>8a</b>	-(CH <sub>2</sub> ) <sub>5</sub> CH <sub>3</sub>	20.2 $\pm$ 1.03	24.30 $\pm$ 1.38	19.04 $\pm$ 1.28	23.88 $\pm$ 1.37	13.11 $\pm$ 1.11
<b>8b</b>	-(CH <sub>2</sub> ) <sub>7</sub> CH <sub>3</sub>	22.34 $\pm$ 1.34	26.14 $\pm$ 1.41	10.46 $\pm$ 1.02	13.40 $\pm$ 1.12	12.63 $\pm$ 1.10
<b>8c</b>	-(CH <sub>2</sub> ) <sub>11</sub> CH <sub>3</sub>	>50	>50	26.04 $\pm$ 1.28	38.67 $\pm$ 1.58	>50
<b>8d</b>	-(CH <sub>2</sub> ) <sub>13</sub> CH <sub>3</sub>	>50	>50	>50	>50	>50
<b>8e</b>	-(CH <sub>2</sub> ) <sub>5</sub>	28.38 $\pm$ 1.36	>50	25.52 $\pm$ 1.40	>50	18.60 $\pm$ 1.27
<b>9a</b>	C <sub>6</sub> H <sub>5</sub> -	18.41 $\pm$ 1.26	44.01 $\pm$ 1.64	20.01 $\pm$ 1.24	26.35 $\pm$ 1.42	22.23 $\pm$ 1.34
<b>9b</b>	2-CF <sub>3</sub> -C <sub>6</sub> H <sub>4</sub> -	>50	>50	34.81 $\pm$ 1.54	>50	>50
<b>9c</b>	2-Cl-C <sub>6</sub> H <sub>4</sub> -	>50	>50	20.43 $\pm$ 1.31	>50	>50
<b>9d</b>	2-OCH <sub>3</sub> -C <sub>6</sub> H <sub>4</sub> -	>50	>50	14.14 $\pm$ 1.23	>50	>50
<b>9e</b>	2-OCH <sub>2</sub> CH <sub>3</sub> -C <sub>6</sub> H <sub>4</sub> -	>50	>50	26.23 $\pm$ 1.41	>50	>50
<b>9f</b>	2-CH <sub>3</sub> -C <sub>6</sub> H <sub>4</sub> -	27.05 $\pm$ 1.43	37.53 $\pm$ 1.57	36.94 $\pm$ 1.56	27.53 $\pm$ 1.14	24.36 $\pm$ 1.38
<b>9g</b>	3-CF <sub>3</sub> -C <sub>6</sub> H <sub>4</sub> -	11.14 $\pm$ 1.04	15.32 $\pm$ 1.18	12.94 $\pm$ 1.02	11.68 $\pm$ 0.45	15.06 $\pm$ 1.17
<b>9h</b>	3-Cl-C <sub>6</sub> H <sub>4</sub> -	18.02 $\pm$ 1.25	25.12 $\pm$ 1.40	13.42 $\pm$ 0.37	19.89 $\pm$ 1.17	14.56 $\pm$ 1.16
<b>9i</b>	3-Br-C <sub>6</sub> H <sub>4</sub> -	22.12 $\pm$ 1.34	25.57 $\pm$ 1.40	8.68 $\pm$ 0.77	18.31 $\pm$ 1.26	23.68 $\pm$ 1.37
<b>9j</b>	3-NO <sub>2</sub> -C <sub>6</sub> H <sub>4</sub> -	31.54 $\pm$ 1.49	>50	13.53 $\pm$ 1.13	>50	>50
<b>9k</b>	4-F-C <sub>6</sub> H <sub>4</sub> -	15.02 $\pm$ 1.17	36.29 $\pm$ 1.56	7.07 $\pm$ 0.63	19.53 $\pm$ 1.29	9.62 $\pm$ 0.98
<b>9l</b>	4-Cl-C <sub>6</sub> H <sub>4</sub> -	15.05 $\pm$ 1.56	21.49 $\pm$ 1.33	7.11 $\pm$ 0.42	14.12 $\pm$ 1.28	16.76 $\pm$ 1.27
<b>9m</b>	4-NO <sub>2</sub> -C <sub>6</sub> H <sub>4</sub> -	8.67 $\pm$ 0.93	17.92 $\pm$ 1.25	7.90 $\pm$ 0.75	16.62 $\pm$ 1.22	8.17 $\pm$ 0.91
<b>9n</b>	4-CF <sub>3</sub> -C <sub>6</sub> H <sub>4</sub> -	5.46 $\pm$ 1.02	5.10 $\pm$ 0.85	7.88 $\pm$ 0.86	7.56 $\pm$ 0.05	6.17 $\pm$ 0.79
<b>9o</b>	4-CH <sub>3</sub> -C <sub>6</sub> H <sub>4</sub> -	>50	>50	21.12 $\pm$ 1.32	34.56 $\pm$ 1.53	36.11 $\pm$ 1.27
<b>9p</b>	4-OCH <sub>3</sub> -C <sub>6</sub> H <sub>4</sub> -	15.73 $\pm$ 1.19	47.19 $\pm$ 1.67	16.70 $\pm$ 1.22	23.49 $\pm$ 1.37	13.79 $\pm$ 1.14
<b>9q</b>	4-OCH <sub>2</sub> CH <sub>3</sub> -C <sub>6</sub> H <sub>4</sub> -	23.03 $\pm$ 1.36	>50	32.05 $\pm$ 1.62	33.03 $\pm$ 1.59	36.98 $\pm$ 1.56
<b>9r</b>	2,4-OCH <sub>3</sub> -C <sub>6</sub> H <sub>3</sub> -	>50	>50	32.48 $\pm$ 1.51	>50	>50
<b>9s</b>	2,5-OCH <sub>3</sub> -C <sub>6</sub> H <sub>3</sub> -	16.12 $\pm$ 1.20	6.99 $\pm$ 0.84	>50	>50	8.58 $\pm$ 0.93
<b>9t</b>	3,4-OCH <sub>3</sub> -C <sub>6</sub> H <sub>3</sub> -	18.85 $\pm$ 1.27	>50	14.08 $\pm$ 1.14	17.94 $\pm$ 1.25	16.26 $\pm$ 1.21
<b>9u</b>	3-Cl-4-F-C <sub>6</sub> H <sub>3</sub> -	14.51 $\pm$ 1.14	22.97 $\pm$ 1.36	18.60 $\pm$ 1.27	14.66 $\pm$ 1.16	>50
<b>9v</b>	3,4,5-OCH <sub>3</sub> -C <sub>6</sub> H <sub>2</sub> -	>50	>50	7.37 $\pm$ 0.86	13.99 $\pm$ 1.14	8.24 $\pm$ 0.91
<b>Gefitinib</b> <sup>b</sup>	-	8.72 $\pm$ 1.10	7.34 $\pm$ 0.86	7.99 $\pm$ 0.54	12.44 $\pm$ 0.87	8.82 $\pm$ 0.63

<sup>a</sup> Cells were treated with different concentrations of the compounds for 72h. IC<sub>50</sub> values are the Mean  $\pm$  SD of three separate experiments. <sup>b</sup> Positive control.

In order to explore the structure-activity relationship, different substituents were introduced to quinazoline scaffold. As shown in Table 1, most of compounds exerted moderate to excellent cytotoxic activity against five human cancer cells. Especially, compound **9n** showed the most excellent cytotoxicity against the tested cells (MDA-MB-231, MCF-7, PC-3, HGC-27 and MGC-803) with IC<sub>50</sub> values of 5.46 $\pm$ 1.02 $\mu$ M, 5.10 $\pm$ 0.85 $\mu$ M, 7.88 $\pm$ 0.86 $\mu$ M, 7.56 $\pm$ 0.05 $\mu$ M and 6.17 $\pm$ 0.79 $\mu$ M, respectively. Comparing **9k-n** with **9o-q**, we concluded that compounds with electron-withdrawing groups at 4-position of benzene exhibited better bioactivity than compounds with electron-donating groups. From

the bioactivity data of compounds **9b-f**, the results revealed that the substituent at 2-position of benzene had little cytotoxic activity for cancer cells. At the same time, comparing **8a-e** with **9k-n**, the results indicated that electron-withdrawing groups at 4-position of benzene was favorable for the antitumor activity. Among all target compounds, compound **9n** exhibited the most excellent growth inhibition activity against breast cancer cells. Therefore, in order to investigate the mechanism of these series of compounds, compound **9n** and breast cancer cells (MDA-MB-231 and MCF-7) were selected for further study.

### **2.2.2 Compound 9n suppressed the proliferation of MDA-MB-231 and MCF-7 cells**

We firstly investigated the impact of compound **9n** on cell viability in MDA-MB-231 and MCF-7 cells by MTT assay for 24, 48 and 72h, respectively. As displayed in Fig. 2A, the cell viability significantly decreased with the delay of time and the increase of compound concentration. The results suggested that compound **9n** could inhibit cell proliferation in a time-dependent and dose-dependent manner. Then, we explored the effect of compound **9n** on the cell proliferation by colony formation assay. As shown in Fig. 2B, the cells treated with 9 $\mu$ M of compound **9n** formed fewer and smaller colonies than the control group. It is demonstrated that compound **9n** inhibited the proliferation of MDA-MB-231 and MCF-7 cells in a dose-dependent manner. As described in Fig. 2C and 2D, the percentage of MDA-MB-231 cells in G1 phase increased from 49.17% to 69.54% after treatment of compound **9n** with 3, 6 and 12 $\mu$ M for 24h. The percentage of MCF-7 cells in G1 phase increased from 52.21% to 75.03%, indicating that compound **9n** inhibited the proliferation of cells by inducing cell cycle arrest in G1 phase. Finally, scratch assay was used to explore whether compound **9n** can inhibit the migration of tumor cells. As presented in Fig. 2E, a marked decrease in scratch-repaired capacity of the cells was observed as the concentration of the compound **9n** increased, which revealed that migration of MDA-MB-231 and MCF-7 cells was inhibited in a dose-dependent manner after 72h of compound **9n** administration.

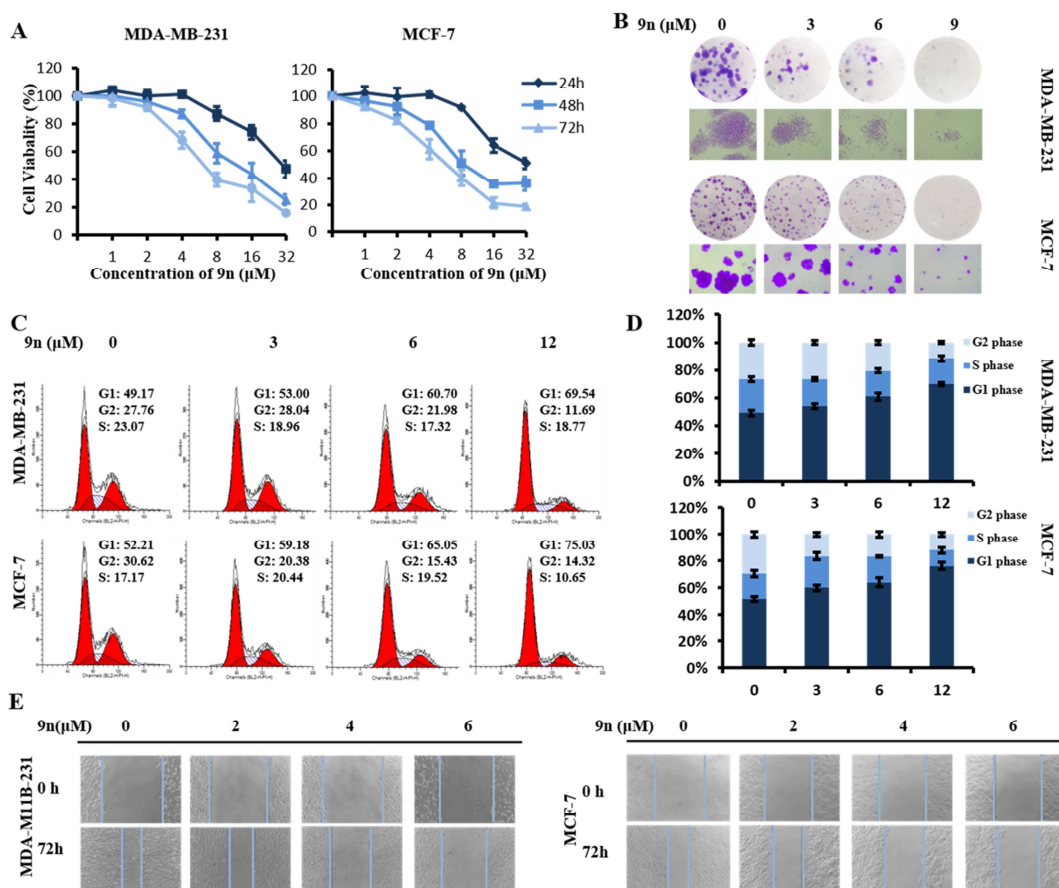
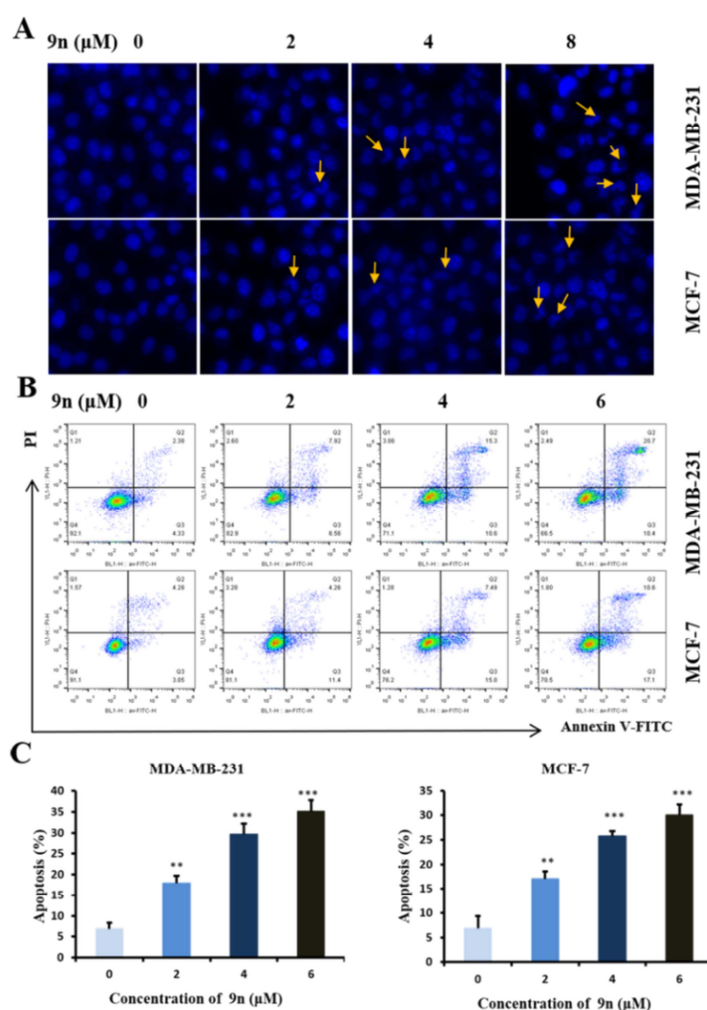


**Fig. 2** Compound **9n** inhibited the proliferation of MDA-MB-231 and MCF-7 cells. (A) The viability of MDA-MB-231 and MCF-7 cells after treatment with different concentration of compound **9n** for 24, 48 and 72h, respectively. (B) MDA-MB-231 and MCF-7 cells were treated with compound **9n** at concentrations of 0, 3, 6 and 9 $\mu\text{M}$  for 7 days; (C) Effect of compound **9n** on cell cycle in MDA-MB-231 and MCF-7 cells; (D) Quantitative analysis of the percentage of MDA-MB-231 and MCF-7 cells cycle phase distribution; (E) Scratch assay of MDA-MB-231 and MCF-7 cells with different concentrations of compound **9n** (magnification, 100). Three individual experiments were performed for each group. The data was expressed as the Mean  $\pm$  SD.

### 2.2.3 Compound **9n** induced MDA-MB-231 and MCF-7 cells apoptosis

Apoptosis is considered a major way that most of the anti-cancer drugs kill tumor cells. Therefore, we determined the effect of compound **9n** on apoptosis of MDA-MB-231 and MCF-7 cells using DAPI staining. The number of apoptotic morphological changes was significantly increased after treatment with the indicated concentration of compound **9n** for 48h (Fig. 3A). Then, in order to better characterize the mode of apoptosis induced by compound **9n**, we performed a biparametric cytofluorimetric analysis using cell apoptosis detection kit, Propidium Iodide (PI) and Annexin V-FITC. The results showed that the percentage of apoptotic cells in MDA-MB-231 cells increased from 6.71%

to 31.1% and the percentage of apoptotic cells in MCF-7 cells increased from 7.33 % to 27.7 % after incubation with compound **9n** for 48h (Fig. 3B & 3C), suggesting that compound **9n** induced the cellular apoptosis in a dose dependent manner. Meanwhile, western blot analysis was performed to examine the expression of apoptosis related proteins (Fig. 3D). After treatment with compound **9n**, the expression of anti-apoptotic protein Bcl-2 was significantly decreased and the pro-apoptotic proteins Bax and p53 were up-regulated both in MDA-MB-231 and MCF-7 cells (Fig. 3E). Finally, it was noteworthy that accumulation of intracellular reactive oxygen species (ROS) can lead to apoptotic cell death, and have direct effect on cellular structure and function [29]. Therefore, we detected the production of intracellular ROS using a fluorescent probe, DHE. The results revealed that the accumulation of ROS increased markedly with the increase of compound **9n** concentration for 48h (Fig. 3F). These data suggested that compound **9n** induced MDA-MB-231 and MCF-7 cells apoptosis through the activation of intrinsic apoptotic pathway.



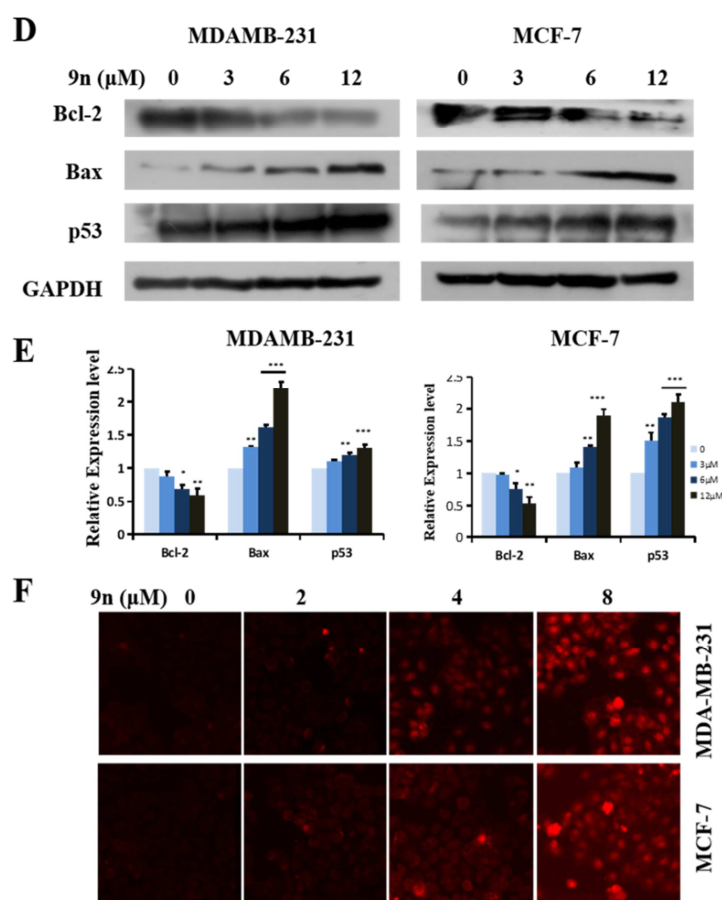


**Fig. 3** Compound **9n** induced apoptosis in MDA-MB-231 and MCF-7 cells. (A) The morphology of the nuclei of MDA-MB-231 and MCF-7 cells was analyzed by DAPI staining (magnification, 100). Yellow arrow indicates nuclear lysis; (B) MDA-MB-231 and MCF-7 cells apoptosis was detected by Annexin V-FITC/PI on flow cytometry after treatment with compound **9n** at different concentrations; (C) Statistical histogram of apoptotic cells of MDA-MB-231 and MCF-7 cells. The data was expressed as the Mean  $\pm$  SD. \* $p < 0.05$ , \*\* $P < 0.01$ , \*\*\* $p < 0.001$  compared with the control group; (D) Western blotting analysis of the effect of compound **9n** intervention on the expression of Bcl-2, Bax and p53 in MDA-MB-231 and MCF-7 cells after treatment with compound **9n** at a concentration of 3, 6, 12 $\mu$ M for 48h. GAPDH was used as control; (E) Histograms of statistical analysis of expression levels of Bax, Bcl-2 and p53 in MDA-MB-231 and MCF-7 cells. (\* $p < 0.05$ , \*\* $P < 0.01$ , \*\*\* $p < 0.001$  compared with the control group). (F) Detection of intracellular reactive oxygen species (ROS) in MDA-MB-231 and MCF-7 cells (magnification, 100). Results were expressed as percentages of control and presented as Mean $\pm$ SD for three independent experiments.

#### 2.2.4 The effect of compound **9n** on EGFR-PI3K signaling pathways

To further explore the mechanism of cytotoxicity of compound **9n** in MDA-MB-231 and MCF-7

cells, the effect of compound **9n** on the expression of EGFR and its downstream protein was investigated (Fig. 4A and 4B). As the concentration of compound **9n** applied to human breast cancer cells (MDA-MB-231 and MCF-7) increased, the expression of phospho-EGFR decreased in a dose-dependent manner, but the total amount of EGFR protein expression was unchanged. Similarly, the expression levels of phospho-PI3K and phospho-AKT were also down-regulated in a dose-dependent manner, while the total PI3K and AKT protein expression levels did not change. These data indicated that compound **9n** regulated MDA-MB-231 and MCF-7 cells via the EGFR-PI3K signaling pathway.

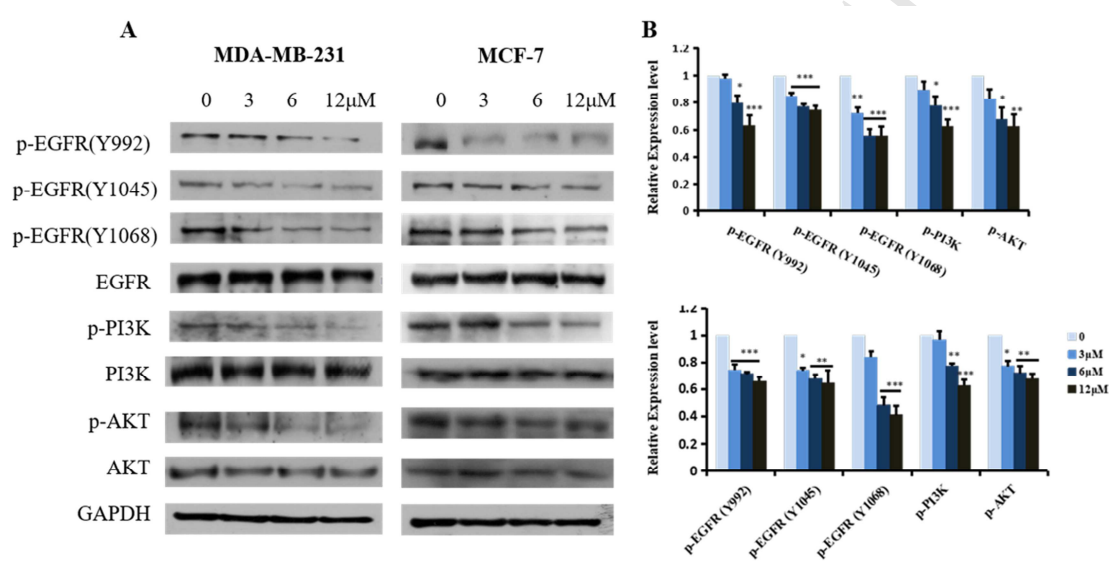


**Fig. 4** The effect of compound **9n** on the EGFR-PI3K signaling pathway. (A) The MDA-MB-231 and MCF-7 cells were stimulated with different concentration (0, 3, 6, 12  $\mu$ M) of compound **9n** for 8h and then subjected to western blot analysis using the indicated antibodies. (B) Quantitative analysis of the proteins level. (\* $p < 0.05$ , \*\* $p < 0.01$ , \*\*\* $p < 0.001$  compared with the control group). Results were expressed as percentages of control and presented as Mean  $\pm$  SD for three independent experiments.

### 2.2.5 Molecular docking study

In order to predict the possible binding mode of compound **9n** with EGFR and PI3K and to explain the activity discrepancy of compounds (8a-e and 9a-v), molecular docking study was carried out using Molecular Operating Environment (MOE) 2014. EGFR (PDB code: 2ITO) and PI3K (PDB code: 3APC) were retrieved from the Protein Data Bank (<http://www.rcsb.org/pdb>) for the docking calculations. Compounds **9n** (the most potent compound), **8a** (the moderately potent) and **9r** (least potent compound) were selected as ligands. To verify the reliability of the docking, we first re-docked

the co-crystallized into the original protein (2ITO). The RMSD between crystal structure and docked structure was 1.0 Å, which indicated that the docking was reliable (Fig. S1). As shown in Fig. 5A, compound **9n** interacted with residues Lys745, Cys797 and Leu781 by  $\pi$ -H interaction, respectively. The NH of compound **9n** formed a hydrogen bond with Asp855 (2.06 Å), indicating that compound **9n** could tightly contact with EGFR. The docking result (Fig. 5B) showed that compound **9n** formed hydrogen bonds with Lys 833 (2.36 Å), Lys 890 (2.30 Å) and Asp 836 (2.63 Å), respectively. The benzene ring of aniline interacted with Tyr 867 through  $\pi$ -H interaction. Comparing the docking results of compounds **8a** (Fig. 5C) and **9n** with PI3K, we found that compound **9n** interacted with Tyr 867 through  $\pi$ -H interaction and **8a** did not. This computational result gave a reasonable explanation for the lack of activity of compound **8a** and also indicated that the aniline with an electron-withdrawing group at 4-position was slightly favorable than fatty amine for the antitumor activity. The lacking interaction with Lys 890 and Tyr 867, which may result in the poor antitumor activity of compound **9r** (Fig. 5D). The docking results were consistent with the biological results.

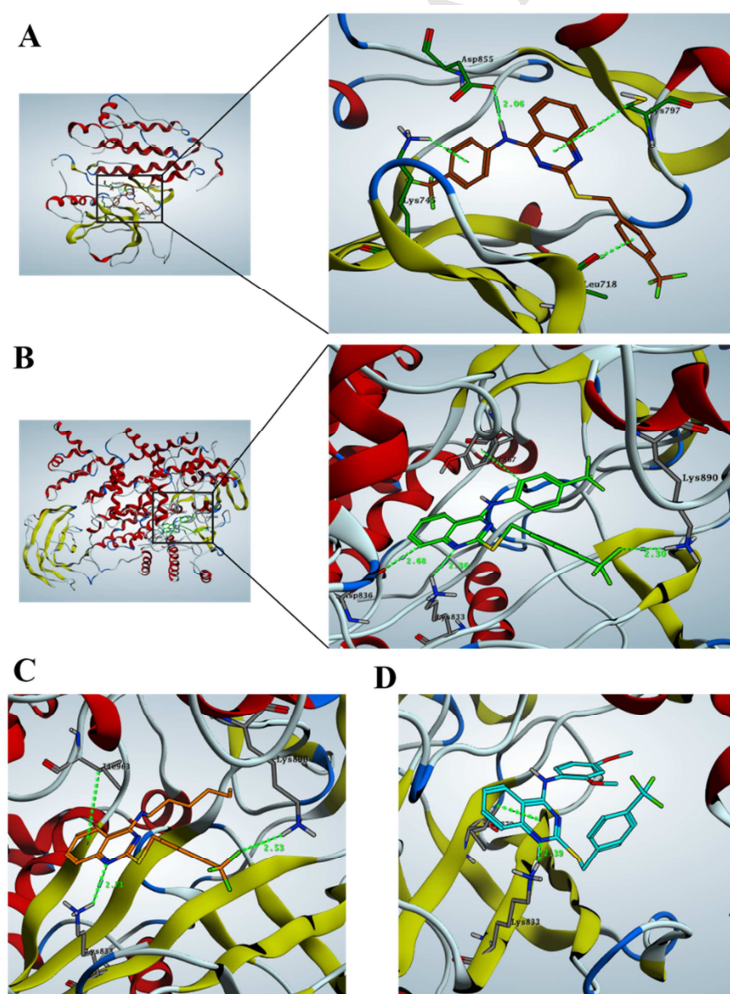


**Fig. 5** (A) Predicted binding model of compound **9n** (dark red) with EGFR (Docking score *S* is -10.2104). (B)

Predicted binding model of compound **9n** (green) with PI3K (Docking score S is -11.1432). (C) Predicted binding model of compound **8a** (orange) with PI3K (Docking score S is -10.0910). (D) Predicted binding model of compound **9r** (cyan) with PI3K (Docking score S is -9.7324). The interacting residues were displayed in sticks. Hydrogen bonds and  $\pi$ -H interaction were shown in green dashed lines.

### 3. Conclusion

In conclusion, a series of novel 2,4-disubstituted quinazolines were synthesized and evaluated for their cytotoxic activity against MDA-MB-231, MCF-7, PC-3, HGC-27 and MGC-803 cells using MTT assay. Among all the tested compounds, compound **9n** showed the most potent anti-proliferative activity against the tested cells, especially for breast cancer cells (MDA-MB-231 and MCF-7). Moreover, cell survival assay, clone formation assay and scratch assay analysis indicated that compound **9n** inhibited cell proliferation and migration, Furthermore, cell cycle experiments showed that compound **9n** induced cell cycle arrest at G1 phase. Meanwhile, DAPI staining, apoptosis, detection of apoptotic protein expression and ROS experiments together suggested that compound **9n** induced apoptosis of MDA-MB-231 and MCF-7 cells through the activation of intrinsic apoptotic pathway. Finally, western blot and molecular docking study analysis indicated that compound **9n** regulated MDA-MB-231 and MCF-7 cells function via the EGFR-PI3K signaling pathway. All the findings suggest that compound **9n** might be a valuable lead compound for anti-tumor agents targeting breast cancer cells.

### 4. Experimental section

#### 4.1. General procedure

Reagents and solvents were purchased from commercial sources and were used without further purification.  $^1\text{H}$  NMR and  $^{13}\text{C}$  NMR spectra were recorded on a Bruker 400 MHz and 101 MHz spectrometer respectively. High resolution mass spectra (HRMS) were recorded on a Waters Micromass Q-T of Micromass spectrometer by electrospray ionization (ESI). Melting points were determined on an X-5 micromelting apparatus. Reactions were monitored by thin-layer chromatography (TLC) on 0.25mm silicagel plates (GF254).

#### 4.2 General procedure for the synthesis of compounds **5** and **6**

Compound **5** and **6** were synthesized according to the literature [30, 31],  $^1\text{H}$  NMR and  $^{13}\text{C}$  NMR spectra of compounds (**5,6**) were in accordance with the published data.

#### 4.3 General procedure for the synthesis of compound **7**

Compound **6** (1.5 mmol) was added to 5 mL of phosphorus oxychloride and then heated to 65 °C for 1h. Then, the mixture was concentrated under reduced pressure and purified by column chromatography (PE:EA = 2:1) to give compound **7**.

4-Chloro-2-((4-(trifluoromethyl)benzyl)thio)quinazoline (**7**). White solid, 65.2% yield, Mp 100.7-101.2 °C. <sup>1</sup>H NMR (400 MHz, DMSO-d<sub>6</sub>) δ (ppm) 8.04 (dd, *J* = 7.9, 1.2 Hz, 1H, Ar-H), 7.80 (d, *J* = 7.4 Hz, 1H, Ar-H), 7.74 (d, *J* = 8.2 Hz, 2H, Ar-H), 7.68 (d, *J* = 7.8 Hz, 2H, Ar-H), 7.62 (d, *J* = 8.1 Hz, 1H, Ar-H), 7.44 (t, *J* = 7.4 Hz, 1H, Ar-H), 4.59 (s, 2H SCH<sub>2</sub>). <sup>13</sup>C NMR (101 MHz, DMSO-d<sub>6</sub>) δ (ppm) 161.09, 154.76, 148.08, 142.79, 134.62, 129.95, 127.90, 127.58, 126.00, 125.75, 125.15, 122.83, 119.97, 32.76. HR-MS (ESI) calcd for C<sub>16</sub>H<sub>10</sub>ClF<sub>3</sub>N<sub>2</sub>S [M+H]<sup>+</sup>: 355.0284, found: 355.0282.

#### 4.4 General procedure for the synthesis of compounds **8a-e**

Compound **7** (1.04 mmol, 2.00 eq) was dissolved in isopropanol (10 ml), then an appropriate amount of amine (1.00 eq) was added, and the mixture was heated to 85 °C for 6h. When the reaction was completed, filtered, dried and the crude product was purified by column chromatography (PE:EA = 1:1) to give compound **8a-e** in 54.7-64.5% yield.

##### 4.4.1. *N*-hexyl-2-((4-(trifluoromethyl)benzyl)thio)quinazolin-4-amine (**8a**)

White solid, 57.7% yield, Mp 91.7-92.0 °C. <sup>1</sup>H NMR (400 MHz, DMSO-d<sub>6</sub>) δ (ppm) 8.38 (t, *J* = 5.2 Hz, 1H, NH), 8.17 (d, *J* = 8.2 Hz, 1H, Ar-H), 7.74 – 7.63 (m, 5H, Ar-H), 7.56 (d, *J* = 8.3 Hz, 1H, Ar-H), 7.39 (t, *J* = 7.6 Hz, 1H, Ar-H), 4.52 (s, 2H, SCH<sub>2</sub>), 3.46 (dd, *J* = 12.9, 6.6 Hz, 2H, CH<sub>2</sub>), 1.56 (dd, *J* = 13.9, 6.9 Hz, 2H, CH<sub>2</sub>), 1.25 (d, *J* = 3.0 Hz, 6H, (CH<sub>2</sub>)<sub>3</sub>), 0.84 (dd, *J* = 12.5, 6.4 Hz, 3H, CH<sub>3</sub>). <sup>13</sup>C NMR (101 MHz, DMSO-d<sub>6</sub>) δ (ppm) 165.58, 158.78, 149.56, 144.34, 132.85, 129.41, 127.49, 127.17, 126.05, 125.00, 124.31, 122.88, 113.05, 40.53, 33.35, 30.96, 28.35, 26.15, 22.00, 13.78. HR-MS (ESI) calcd for C<sub>22</sub>H<sub>24</sub>F<sub>3</sub>N<sub>3</sub>S [M+H]<sup>+</sup>: 420.1721, found: 420.1724.

##### 4.4.2. *N*-octyl-2-((4-(trifluoromethyl)benzyl)thio)quinazolin-4-amine (**8b**)

White solid, 64.5% yield, Mp 92.1-92.6 °C. <sup>1</sup>H NMR (400 MHz, DMSO-d<sub>6</sub>) δ (ppm) 8.37 (t, *J* = 5.4 Hz, 1H, NH), 8.18 (d, *J* = 7.6 Hz, 1H, Ar-H), 7.67 (dd, *J* = 18.9, 8.4 Hz, 5H, Ar-H), 7.59 – 7.53 (m, 1H, Ar-H), 7.42 – 7.36 (m, 1H, Ar-H), 4.52 (s, 2H, SCH<sub>2</sub>), 3.47 (dd, *J* = 13.0, 6.7 Hz, 2H, CH<sub>2</sub>), 3.35 (s, 2H, CH<sub>2</sub>), 1.57 (dd, *J* = 13.9, 7.0 Hz, 2H, CH<sub>2</sub>), 1.22 (dd, *J* = 12.5, 5.9 Hz, 8H, (CH<sub>2</sub>)<sub>4</sub>), 0.82 (t, *J* = 6.8 Hz, 3H, CH<sub>3</sub>). <sup>13</sup>C NMR (101 MHz, DMSO-d<sub>6</sub>) δ (ppm) 165.57, 158.77, 149.57, 144.35, 132.85, 129.41, 127.49, 127.17, 126.05, 125.00, 124.31, 122.88, 113.04, 40.51, 33.34, 31.18, 28.68, 28.60, 28.36, 26.46, 22.00, 13.82. HR-MS (ESI) calcd for C<sub>24</sub>H<sub>28</sub>F<sub>3</sub>N<sub>3</sub>S [M+H]<sup>+</sup>: 448.2034, found: 448.2032.

##### 4.4.3. *N*-dodecyl-2-((4-(trifluoromethyl)benzyl)thio)quinazolin-4-amine (**8c**)

White solid, 58.3% yield, Mp 71.8-72.0 °C. <sup>1</sup>H NMR (400 MHz, DMSO-d<sub>6</sub>) δ (ppm) 8.40 (s, 1H,

NH), 8.17 (d,  $J = 8.1$  Hz, 1H, Ar-H), 7.67 (dd,  $J = 12.1, 6.7$  Hz, 5H, Ar-H), 7.55 (d,  $J = 8.3$  Hz, 1H, Ar-H), 7.39 (t,  $J = 7.6$  Hz, 1H, Ar-H), 4.52 (s, 2H, SCH<sub>2</sub>), 3.47 (dd,  $J = 12.9, 6.6$  Hz, 2H, CH<sub>2</sub>), 1.57 (dd,  $J = 13.7, 6.8$  Hz, 2H, CH<sub>2</sub>), 1.22 (d,  $J = 21.9$  Hz, 18H, (CH<sub>2</sub>)<sub>9</sub>), 0.83 (t,  $J = 6.8$  Hz, 3H, CH<sub>3</sub>). <sup>13</sup>C NMR (101 MHz, DMSO-d<sub>6</sub>)  $\delta$  (ppm) 165.54, 158.76, 149.43, 144.30, 132.89, 130.02, 129.41, 127.35, 125.95, 125.00, 124.34, 122.89, 113.01, 40.50, 33.34, 31.23, 28.93, 28.62, 28.33, 26.43, 22.02, 13.85. HR-MS (ESI) calcd for C<sub>28</sub>H<sub>36</sub>F<sub>3</sub>N<sub>3</sub>S [M+H]<sup>+</sup>: 504.2660, found: 504.2662.

#### 4.4.4. *N-tetradecyl-2-((4-(trifluoromethyl)benzyl)thio)quinazolin-4-amine (8d)*

White solid, 59.1% yield, Mp 76.4-76.9 °C. <sup>1</sup>H NMR (400 MHz, DMSO-d<sub>6</sub>)  $\delta$  (ppm) 8.38 (t,  $J = 5.0$  Hz, 1H, NH), 8.17 (d,  $J = 8.2$  Hz, 1H, Ar-H), 7.66 (dd,  $J = 20.7, 8.4$  Hz, 5H, Ar-H), 7.55 (d,  $J = 8.3$  Hz, 1H, Ar-H), 7.38 (t,  $J = 7.5$  Hz, 1H, Ar-H), 4.52 (s, 2H, SCH<sub>2</sub>), 3.47 (dd,  $J = 12.7, 6.4$  Hz, 2H, CH<sub>2</sub>), 1.64 – 1.50 (m, 2H, CH<sub>2</sub>), 1.21 (d,  $J = 25.5$  Hz, 22H, (CH<sub>2</sub>)<sub>11</sub>), 0.83 (t,  $J = 6.6$  Hz, 3H, CH<sub>3</sub>). <sup>13</sup>C NMR (101 MHz, DMSO-d<sub>6</sub>)  $\delta$  (ppm) 165.56, 158.77, 149.52, 144.25, 132.76, 129.35, 127.53, 127.21, 125.97, 124.95, 124.22, 122.86, 113.05, 40.50, 33.37, 31.23, 28.95, 28.65, 28.36, 26.46, 22.02, 13.78. HR-MS (ESI) calcd for C<sub>30</sub>H<sub>40</sub>F<sub>3</sub>N<sub>3</sub>S [M+H]<sup>+</sup>: 532.2973, found: 532.2975.

#### 4.4.5. *N-cyclopentyl-2-((4-(trifluoromethyl)benzyl)thio)quinazolin-4-amine(8e)*

Oily liquid, 54.7% yield. <sup>1</sup>H NMR (400 MHz, DMSO-d<sub>6</sub>)  $\delta$  (ppm) 8.29 (d,  $J = 7.6$  Hz, 1H, NH), 8.12 – 8.05 (m, 1H, Ar-H), 7.73 – 7.69 (m, 3H, Ar-H), 7.66 (d,  $J = 8.4$  Hz, 2H, Ar-H), 7.60 – 7.54 (m, 1H, Ar-H), 7.42 – 7.35 (m, 1H, Ar-H), 4.52 (s, 2H, SCH<sub>2</sub>), 3.37 (s, 1H, CH), 1.99 – 1.90 (m, 2H, CH<sub>2</sub>), 1.79 – 1.68 (m, 2H, CH<sub>2</sub>), 1.67 – 1.49 (m, 4H, (CH<sub>2</sub>)<sub>2</sub>). <sup>13</sup>C NMR (101 MHz, DMSO-d<sub>6</sub>)  $\delta$  (ppm) 165.55, 158.47, 149.56, 144.32, 132.82, 129.42, 127.47, 127.15, 125.98, 125.03, 124.16, 123.23, 113.02, 52.17, 33.44, 31.79, 23.65. HR-MS (ESI) calcd for C<sub>21</sub>H<sub>20</sub>F<sub>3</sub>N<sub>3</sub>S [M+H]<sup>+</sup>: 404.1408, found: 404.1407.

### 4.5 General procedure for the synthesis of compounds 9a-v

Compound **7** (2.00 eq) was dissolved in N,N-Dimethylformamide(DMF), then an appropriate amount of aromatic amines (1.50 eq) was added, and the mixture was heated to 90 °C for 4h. When the reaction was completed, filtered, dried and the crude product was purified by column chromatography (PE:EA = 1:1 ~ 1.5:1) to give compound **9a-v** in 55.3-84.2% yield.

#### 4.5.1 *N-phenyl-2-((4-(trifluoromethyl)benzyl)thio)quinazolin-4-amine (9a)*

White solid, 63.8% yield, Mp 144.2-144.9 °C. <sup>1</sup>H NMR (400 MHz, DMSO-d<sub>6</sub>)  $\delta$  (ppm) 9.91 (s, 1H, NH), 8.48 (d,  $J = 8.1$  Hz, 1H, Ar-H), 7.81 (t,  $J = 7.6$  Hz, 1H, Ar-H), 7.75 (d,  $J = 7.7$  Hz, 2H, Ar-H), 7.67 (d,  $J = 8.2$  Hz, 1H, Ar-H), 7.60 (q,  $J = 8.6$  Hz, 4H, Ar-H), 7.52 (t,  $J = 7.2$  Hz, 1H, Ar-H), 7.40 (t,  $J = 7.9$  Hz, 2H, Ar-H), 7.16 (t,  $J = 7.4$  Hz, 1H, Ar-H), 4.47 (s, 2H, SCH<sub>2</sub>). <sup>13</sup>C NMR (101 MHz, DMSO-d<sub>6</sub>)  $\delta$  (ppm) 165.26, 157.29, 150.18, 143.96, 138.60, 133.49, 129.57, 128.45, 127.51, 127.19, 126.35, 125.58,

125.01, 124.27, 123.26, 122.97, 113.11, 33.34. HR-MS (ESI) calcd for  $C_{22}H_{16}F_3N_3S$   $[M+H]^+$ : 412.1095, found: 412.1097.

#### 4.5.2. 2-((4-(Trifluoromethyl)benzyl)thio)-N-(2-(trifluoromethyl)phenyl)quinazolin-4-amine (9b)

White solid, 60.2% yield, Mp 116.4-117.1 °C.  $^1H$  NMR (400 MHz, DMSO- $d_6$ )  $\delta$  (ppm) 10.02 (s, 1H, NH), 8.40 (d,  $J$  = 8.1 Hz, 1H, Ar-H), 7.87 (d,  $J$  = 8.2 Hz, 1H, Ar-H), 7.82 – 7.76 (m, 2H, Ar-H), 7.66 – 7.61 (m, 3H, Ar-H), 7.52 (d,  $J$  = 8.1 Hz, 3H, Ar-H), 7.29 (d,  $J$  = 8.0 Hz, 2H, Ar-H), 4.20 (s, 2H,  $SCH_2$ ).  $^{13}C$  NMR (101 MHz, DMSO- $d_6$ )  $\delta$  (ppm) 165.32, 159.43, 150.18, 144.13, 136.30, 134.89, 133.66, 133.26, 131.96, 129.25, 127.83, 127.34, 126.91, 126.73, 126.19, 125.10, 124.81, 123.22, 115.28, 112.53, 33.09. HR-MS (ESI) calcd for  $C_{23}H_{15}F_6N_3S$   $[M+H]^+$ : 480.0969, found: 480.0967.

#### 4.5.3. N-(2-chlorophenyl)-2-((4-(trifluoromethyl)benzyl)thio)quinazolin-4-amine (9c)

White solid, 63.4% yield, Mp 163.6-163.9 °C.  $^1H$  NMR (400 MHz, DMSO- $d_6$ )  $\delta$  (ppm) 11.92 (s, 1H, NH), 8.81 (d,  $J$  = 8.2 Hz, 1H, Ar-H), 8.01 (t,  $J$  = 7.7 Hz, 1H, Ar-H), 7.88 (d,  $J$  = 8.3 Hz, 1H, Ar-H), 7.72 (t,  $J$  = 8.0 Hz, 2H, Ar-H), 7.67 (d,  $J$  = 7.7 Hz, 1H, Ar-H), 7.60 – 7.41 (m, 4H, Ar-H), 7.13 (t,  $J$  = 17.2 Hz, 2H, Ar-H), 4.29 (s, 2H,  $SCH_2$ ).  $^{13}C$  NMR (101 MHz, DMSO- $d_6$ )  $\delta$  (ppm) 164.16, 158.55, 142.30, 136.03, 134.22, 131.11, 130.00, 129.83, 129.56, 129.30, 128.01, 127.80, 127.48, 127.08, 125.45, 124.96, 124.83, 119.72, 111.34, 32.97. HR-MS (ESI) calcd for  $C_{22}H_{15}ClF_3N_3S$   $[M+H]^+$ : 446.0706, found: 446.0698.

#### 4.5.4. N-(2-methoxyphenyl)-2-((4-(trifluoromethyl)benzyl)thio)quinazolin-4-amine (9d)

White solid, 69.5% yield, Mp 152.5-153.5 °C.  $^1H$  NMR (400 MHz, DMSO- $d_6$ )  $\delta$  (ppm) 9.61 (s, 1H, NH), 8.40 (d,  $J$  = 7.9 Hz, 1H, Ar-H), 7.81 – 7.75 (m, 1H, Ar-H), 7.62 (d,  $J$  = 7.8 Hz, 1H, Ar-H), 7.59 – 7.52 (m, 3H, Ar-H), 7.51 – 7.46 (m, 1H, Ar-H), 7.38 (d,  $J$  = 8.1 Hz, 2H, Ar-H), 7.34 – 7.27 (m, 1H, Ar-H), 7.18 (d,  $J$  = 7.4 Hz, 1H, Ar-H), 7.04 (td,  $J$  = 7.6, 1.1 Hz, 1H, Ar-H), 4.30 (s, 2H,  $SCH_2$ ), 3.80 (s, 3H,  $OCH_3$ ).  $^{13}C$  NMR (101 MHz, DMSO- $d_6$ )  $\delta$  (ppm) 165.40, 158.20, 153.90, 150.15, 144.34, 133.37, 129.51, 127.73, 127.27, 127.02, 126.61, 126.19, 125.60, 124.88, 124.85, 123.23, 120.22, 112.89, 111.93, 55.56, 33.17. HR-MS (ESI) calcd for  $C_{23}H_{18}F_3N_3OS$   $[M+H]^+$ : 442.1201, found: 442.1200.

#### 4.5.5. N-(2-ethoxyphenyl)-2-((4-(trifluoromethyl)benzyl)thio)quinazolin-4-amine (9e)

White solid, 70.4% yield, Mp 159.8-160.3 °C.  $^1H$  NMR (400 MHz, DMSO- $d_6$ )  $\delta$  (ppm) 11.33 (s, 1H, NH), 8.68 (d,  $J$  = 8.3 Hz, 1H, Ar-H), 7.98 (t,  $J$  = 7.7 Hz, 1H, Ar-H), 7.80 (d,  $J$  = 8.4 Hz, 1H, Ar-H), 7.69 (t,  $J$  = 7.6 Hz, 1H, Ar-H), 7.53 – 7.47 (m, 3H, Ar-H), 7.42 (t,  $J$  = 7.8 Hz, 1H, Ar-H), 7.27 (d,  $J$  = 8.2 Hz, 1H, Ar-H), 7.11 (dd,  $J$  = 14.4, 7.6 Hz, 3H, Ar-H), 4.30 (s, 2H,  $SCH_2$ ), 4.11 (q,  $J$  = 6.9 Hz, 2H,  $OCH_2$ ), 1.21 (t,  $J$  = 6.9 Hz, 3H,  $CH_3$ ).  $^{13}C$  NMR (101 MHz, DMSO- $d_6$ )  $\delta$  (ppm) 163.78, 158.13, 153.46, 142.48, 135.72, 129.49, 129.03, 128.08, 127.72, 127.41, 126.93, 125.45, 125.22, 124.91, 124.66, 122.75, 120.37, 113.20, 111.42, 63.87, 32.94, 14.55. HR-MS (ESI) calcd for  $C_{24}H_{20}F_3N_3OS$   $[M+H]^+$ : 456.1357, found: 456.1354.

**4.5.6. *N*-(*o*-tolyl)-2-((4-(trifluoromethyl)benzyl)thio)quinazolin-4-amine (9f)**

White solid, 73.0% yield, Mp 179.4-180.2 °C. <sup>1</sup>H NMR (400 MHz, DMSO-*d*<sub>6</sub>) δ (ppm) 11.65 (s, 1H, NH), 8.79 (d, *J* = 8.2 Hz, 1H, Ar-H), 7.99 (t, *J* = 7.7 Hz, 1H, Ar-H), 7.81 (d, *J* = 8.3 Hz, 1H, Ar-H), 7.69 (t, *J* = 7.7 Hz, 1H, Ar-H), 7.47 (t, *J* = 10.1 Hz, 4H, Ar-H), 7.42 – 7.34 (m, 2H, Ar-H), 7.03 (d, *J* = 7.8 Hz, 2H, Ar-H), 4.24 (s, 2H, SCH<sub>2</sub>), 2.25 (s, 3H, CH<sub>3</sub>). <sup>13</sup>C NMR (101 MHz, DMSO-*d*<sub>6</sub>) δ (ppm) 163.92, 158.40, 142.34, 135.83, 135.39, 135.04, 130.75, 129.42, 128.07, 127.82, 127.44, 126.95, 126.52, 125.46, 124.99, 124.87, 122.75, 119.08, 111.48, 32.91, 17.65. HR-MS (ESI) calcd for C<sub>23</sub>H<sub>18</sub>F<sub>3</sub>N<sub>3</sub>S [M+H]<sup>+</sup>: 426.1252, found: 426.1253.

**4.5.7. 2-((4-(Trifluoromethyl)benzyl)thio)-*N*-(3-(trifluoromethyl)phenyl)quinazolin-4-amine (9g)**

White solid, 74.0% yield, Mp 155.5-155.8 °C. <sup>1</sup>H NMR (400 MHz, DMSO-*d*<sub>6</sub>) δ (ppm) 11.71 (s, 1H, NH), 8.87 (d, *J* = 8.3 Hz, 1H, Ar-H), 8.24 (s, 1H, Ar-H), 8.07 (d, *J* = 7.9 Hz, 1H, Ar-H), 7.99 (t, *J* = 7.7 Hz, 1H, Ar-H), 7.85 (d, *J* = 8.3 Hz, 1H, Ar-H), 7.75 – 7.66 (m, 2H, Ar-H), 7.64 (d, *J* = 7.8 Hz, 1H, Ar-H), 7.55 (d, *J* = 8.1 Hz, 2H, Ar-H), 7.39 (d, *J* = 8.0 Hz, 2H, Ar-H), 4.50 (s, 2H, SCH<sub>2</sub>). <sup>13</sup>C NMR (101 MHz, DMSO-*d*<sub>6</sub>) δ (ppm) 164.27, 157.81, 142.03, 138.01, 135.65, 129.90, 129.43, 129.23, 128.52, 127.90, 127.59, 126.74, 125.44, 125.26, 125.02, 124.83, 122.73, 122.56, 121.24, 112.08, 33.19. HR-MS (ESI) calcd for C<sub>23</sub>H<sub>15</sub>F<sub>6</sub>N<sub>3</sub>S [M+H]<sup>+</sup>: 480.0969, found: 480.0969.

**4.5.8. *N*-(3-chlorophenyl)-2-((4-(trifluoromethyl)benzyl)thio)quinazolin-4-amine (9h)**

White solid, 70.1% yield, Mp 156.6-157.2 °C. <sup>1</sup>H NMR (400 MHz, DMSO-*d*<sub>6</sub>) δ (ppm) 11.43 (s, 1H, NH), 8.77 (d, *J* = 7.9 Hz, 1H, Ar-H), 7.96 (dd, *J* = 15.4, 7.8 Hz, 2H, Ar-H), 7.81 (d, *J* = 8.3 Hz, 1H, Ar-H), 7.68 (dd, *J* = 12.0, 8.0 Hz, 2H, Ar-H), 7.59 (d, *J* = 8.1 Hz, 2H, Ar-H), 7.49 (d, *J* = 8.1 Hz, 1H, Ar-H), 7.46 – 7.40 (m, 2H, Ar-H), 7.35 (d, *J* = 8.0 Hz, 1H, Ar-H), 4.51 (s, 2H, SCH<sub>2</sub>). <sup>13</sup>C NMR (101 MHz, DMSO-*d*<sub>6</sub>) δ (ppm) 164.09, 157.76, 141.97, 138.39, 135.79, 132.85, 130.29, 129.48, 127.94, 127.62, 126.85, 126.16, 125.45, 125.06, 124.72, 123.52, 122.75, 119.82, 111.93, 33.19. HR-MS (ESI) calcd for C<sub>22</sub>H<sub>15</sub>ClF<sub>3</sub>N<sub>3</sub>S [M+H]<sup>+</sup>: 446.0706, found: 446.0705.

**4.5.9. *N*-(3-bromophenyl)-2-((4-(trifluoromethyl)benzyl)thio)quinazolin-4-amine (9i)**

White solid, 71.3% yield, Mp 160.3-161.2 °C. <sup>1</sup>H NMR (400 MHz, DMSO-*d*<sub>6</sub>) δ (ppm) 11.62 (s, 1H, NH), 8.88 – 8.79 (m, 1H, Ar-H), 8.08 (d, *J* = 1.7 Hz, 1H, Ar-H), 7.98 (t, *J* = 7.7 Hz, 1H, Ar-H), 7.83 (d, *J* = 8.3 Hz, 1H, Ar-H), 7.74 (d, *J* = 8.1 Hz, 1H, Ar-H), 7.68 (t, *J* = 7.7 Hz, 1H, Ar-H), 7.58 (d, *J* = 8.1 Hz, 2H, Ar-H), 7.50 (d, *J* = 8.1 Hz, 1H, Ar-H), 7.44 (d, *J* = 8.0 Hz, 1H, Ar-H), 7.42 – 7.38 (m, 2H, Ar-H), 4.52 (s, 2H, SCH<sub>2</sub>). <sup>13</sup>C NMR (101 MHz, DMSO-*d*<sub>6</sub>) δ (ppm) 164.12, 157.73, 142.04, 138.58, 135.73, 130.58, 129.52, 128.98, 127.93, 127.48, 126.81, 125.46, 125.08, 124.94, 123.83, 122.76, 121.11, 120.05, 111.97, 33.23. HR-MS (ESI) calcd for C<sub>22</sub>H<sub>15</sub>BrF<sub>3</sub>N<sub>3</sub>S [M+H]<sup>+</sup>: 490.0200, found: 490.0201.

**4.5.10. *N*-(3-nitrophenyl)-2-((4-(trifluoromethyl)benzyl)thio)quinazolin-4-amine (9j)**

White solid, 55.3% yield, Mp 218.8-219.5 °C. <sup>1</sup>H NMR (400 MHz, DMSO-d<sub>6</sub>) δ (ppm) 11.57 (s, 1H, NH), 8.95 – 8.78 (m, 2H, Ar-H), 8.24 (d, J = 8.1 Hz, 1H, Ar-H), 8.08 (d, J = 8.2 Hz, 1H, Ar-H), 7.98 (t, J = 7.7 Hz, 1H, Ar-H), 7.83 (d, J = 8.3 Hz, 1H, Ar-H), 7.70 (dd, J = 17.3, 8.5 Hz, 2H, Ar-H), 7.59 (d, J = 8.2 Hz, 2H, Ar-H), 7.48 (d, J = 8.0 Hz, 2H, Ar-H), 4.56 (s, 2H, SCH<sub>2</sub>). <sup>13</sup>C NMR (101 MHz, DMSO-d<sub>6</sub>) δ (ppm) 164.38, 157.72, 147.71, 141.84, 138.52, 135.60, 130.31, 129.93, 129.47, 127.92, 127.60, 126.71, 125.45, 125.10, 124.84, 122.75, 120.19, 118.68, 112.19, 33.50. HR-MS (ESI) calcd for C<sub>22</sub>H<sub>15</sub>F<sub>3</sub>N<sub>4</sub>O<sub>2</sub>S [M+H]<sup>+</sup>: 457.0946, found: 457.0945.

**4.5.11. *N*-(4-fluorophenyl)-2-((4-(trifluoromethyl)benzyl)thio)quinazolin-4-amine (9k)**

White solid, 71.9% yield, Mp 170.6-171.0 °C. <sup>1</sup>H NMR (400 MHz, DMSO-d<sub>6</sub>) δ (ppm) 9.95 (s, 1H, NH), 8.45 (d, J = 7.7 Hz, 1H, Ar-H), 7.84 – 7.79 (m, 1H, Ar-H), 7.77 – 7.72 (m, 2H, Ar-H), 7.68 – 7.65 (m, 1H, Ar-H), 7.60 (q, J = 8.6 Hz, 4 H, Ar-H), 7.55 – 7.50 (m, 1H, Ar-H), 7.26 – 7.19 (m, 2H, Ar-H), 4.46 (s, 2H, SCH<sub>2</sub>). <sup>13</sup>C NMR (101 MHz, DMSO-d<sub>6</sub>) δ (ppm) 165.23, 160.00, 157.60, 157.34, 150.12, 143.93, 134.89, 133.52, 129.56, 127.52, 126.35, 125.05, 124.97, 123.21, 115.19, 114.97, 113.01, 33.35. HR-MS (ESI) calcd for C<sub>22</sub>H<sub>15</sub>F<sub>4</sub>N<sub>3</sub>S [M+H]<sup>+</sup>: 430.1001, found: 430.1003.

**4.5.12. *N*-(4-chlorophenyl)-2-((4-(trifluoromethyl)benzyl)thio)quinazolin-4-amine (9l)**

White solid, 73.0% yield, Mp 180.0-181.7 °C. <sup>1</sup>H NMR (400 MHz, DMSO-d<sub>6</sub>) δ (ppm) 11.70 (s, 1H, NH), 8.86 (d, J = 8.3 Hz, 1H, Ar-H), 7.98 (t, J = 7.6 Hz, 1H, Ar-H), 7.84 (d, J = 8.3 Hz, 1H, Ar-H), 7.75 (d, J = 8.4 Hz, 2H, Ar-H), 7.68 (t, J = 7.6 Hz, 1H, Ar-H), 7.58 (d, J = 7.9 Hz, 2H, Ar-H), 7.51 (d, J = 8.4 Hz, 2H, Ar-H), 7.39 (d, J = 7.8 Hz, 2H, Ar-H), 4.51 (s, 2H, SCH<sub>2</sub>). <sup>13</sup>C NMR (101 MHz, DMSO-d<sub>6</sub>) δ (ppm) 164.14, 157.69, 142.08, 135.88, 135.65, 130.38, 129.47, 128.59, 128.21, 127.89, 126.77, 126.59, 125.03, 124.87, 124.50, 122.77, 111.98, 33.27. HR-MS (ESI) calcd for C<sub>22</sub>H<sub>15</sub>ClF<sub>3</sub>N<sub>3</sub>S [M+H]<sup>+</sup>: 446.0706, found: 446.0706.

**4.5.13. *N*-(4-nitrophenyl)-2-((4-(trifluoromethyl)benzyl)thio)quinazolin-4-amine (9m)**

White solid, 58.1% yield, Mp 219.7-220.3 °C. <sup>1</sup>H NMR (400 MHz, DMSO-d<sub>6</sub>) δ (ppm) 11.29 (s, 1H, NH), 8.80 (d, J = 7.9 Hz, 1H, Ar-H), 8.26 (d, J = 9.1 Hz, 2H, Ar-H), 8.11 (d, J = 9.1 Hz, 2H, Ar-H), 7.97 (t, J = 7.5 Hz, 1H, Ar-H), 7.83 (d, J = 8.3 Hz, 1H, Ar-H), 7.66 (d, J = 7.4 Hz, 1H, Ar-H), 7.60 (dd, J = 17.7, 8.2 Hz, 4H, Ar-H), 4.58 (s, 2H, SCH<sub>2</sub>). <sup>13</sup>C NMR (101 MHz, DMSO-d<sub>6</sub>) δ (ppm) 164.54, 162.78, 157.51, 150.24, 140.84, 135.39, 134.86, 129.53, 126.87, 126.54, 125.06, 124.74, 124.21, 123.54, 122.23, 115.29, 114.28, 33.54. HR-MS (ESI) calcd for C<sub>22</sub>H<sub>15</sub>F<sub>3</sub>N<sub>4</sub>O<sub>2</sub>S [M+H]<sup>+</sup>: 457.0946, found: 457.0945.

**4.5.14. 2-((4-(Trifluoromethyl)benzyl)thio)-*N*-(4-(trifluoromethyl)phenyl)quinazolin-4-amine (9n)**

White solid, 72.7% yield, Mp 163.5-163.9 °C. <sup>1</sup>H NMR (400 MHz, DMSO-d<sub>6</sub>) δ (ppm) 11.45 (s, 1H, NH), 8.81 (d, J = 8.3 Hz, 1H, Ar-H), 7.98 (s, 1H, Ar-H), 7.95 (d, J = 6.2 Hz, 2H, Ar-H), 7.82 (d, J = 8.3 Hz, 1H, Ar-H), 7.76 (d, J = 8.5 Hz, 2H, Ar-H), 7.67 (t, J = 7.6 Hz, 1H, Ar-H), 7.56 (d, J = 8.1 Hz,

2H, Ar-H), 7.44 (d, J = 8.0 Hz, 2H, Ar-H), 4.52 (s, 2H, SCH<sub>2</sub>). <sup>13</sup>C NMR (101 MHz, DMSO-d<sub>6</sub>) δ (ppm) 164.39, 157.77, 142.10, 140.93, 135.59, 129.37, 128.17, 127.85, 127.53, 126.68, 125.65, 125.46, 125.00, 124.87, 124.73, 122.76, 120.79, 112.19, 33.37. HR-MS (ESI) calcd for C<sub>23</sub>H<sub>15</sub>F<sub>6</sub>N<sub>3</sub>S [M+H]<sup>+</sup>: 480.0969, found: 480.0970.

**4.5.15. *N*-(*p*-tolyl)-2-((4-(trifluoromethyl)benzyl)thio)quinazolin-4-amine (9o)**

White solid, 73.5% yield, Mp 165.1-166.0 °C. <sup>1</sup>H NMR (400 MHz, DMSO-d<sub>6</sub>) δ (ppm) 11.61 (s, 1H, NH), 8.82 (d, J = 8.3 Hz, 1H, Ar-H), 7.96 (t, J = 7.7 Hz, 1H, Ar-H), 7.83 (d, J = 8.3 Hz, 1H, Ar-H), 7.67 (t, J = 7.6 Hz, 1H, Ar-H), 7.58 – 7.55 (m, 2H, Ar-H), 7.54 (s, 1H, Ar-H), 7.32 (d, J = 8.0 Hz, 2H, Ar-H), 7.28 (d, J = 8.2 Hz, 2H, Ar-H), 7.22 – 7.16 (m, 1H, Ar-H), 4.48 (s, 2H, SCH<sub>2</sub>), 2.33 (s, 3H, CH<sub>3</sub>). <sup>13</sup>C NMR (101 MHz, DMSO-d<sub>6</sub>) δ (ppm) 163.91, 157.59, 150.23, 142.06, 140.84, 136.09, 135.65, 134.84, 134.07, 129.52, 129.09, 126.85, 125.03, 122.23, 115.30, 114.27, 111.80, 33.18, 20.58. HR-MS (ESI) calcd for C<sub>23</sub>H<sub>18</sub>F<sub>3</sub>N<sub>3</sub>S [M+H]<sup>+</sup>: 426.1252, found: 426.1253.

**4.5.16. *N*-(4-methoxyphenyl)-2-((4-(trifluoromethyl)benzyl)thio)quinazolin-4-amine (9p)**

White solid, 73.0% yield, Mp 180.2-181.2 °C. <sup>1</sup>H NMR (400 MHz, DMSO-d<sub>6</sub>) δ (ppm) 11.48 (s, 1H, NH), 8.73 (d, J = 8.3 Hz, 1H, Ar-H), 7.96 (t, J = 7.7 Hz, 1H, Ar-H), 7.78 (d, J = 8.3 Hz, 1H, Ar-H), 7.58 (d, J = 4.5 Hz, 2H, Ar-H), 7.55 (d, J = 3.7 Hz, 2H, Ar-H), 7.32 (d, J = 8.0 Hz, 2H, Ar-H), 7.19 (d, J = 7.9 Hz, 1H, Ar-H), 7.02 (d, J = 8.9 Hz, 2H, Ar-H), 4.46 (s, 2H, SCH<sub>2</sub>), 3.78 (s, 3H, OCH<sub>3</sub>). <sup>13</sup>C NMR (101 MHz, DMSO-d<sub>6</sub>) δ (ppm) 163.95, 162.79, 157.82, 157.59, 150.25, 140.82, 134.86, 129.53, 126.87, 126.55, 124.96, 124.62, 122.24, 115.29, 114.28, 113.90, 111.77, 55.31, 33.19. HR-MS (ESI) calcd for C<sub>23</sub>H<sub>18</sub>F<sub>3</sub>N<sub>3</sub>OS [M+H]<sup>+</sup>: 442.1201, found: 442.1201.

**4.5.17. *N*-(4-ethoxyphenyl)-2-((4-(trifluoromethyl)benzyl)thio)quinazolin-4-amine (9q)**

White solid, 65.6% yield, Mp 167.0-167.8 °C. <sup>1</sup>H NMR (400 MHz, DMSO-d<sub>6</sub>) δ (ppm) 11.62 (s, 1H, NH), 8.78 (d, J = 8.3 Hz, 1H, Ar-H), 7.97 (t, J = 7.7 Hz, 1H, Ar-H), 7.80 (d, J = 8.3 Hz, 1H, Ar-H), 7.67 (t, J = 7.5 Hz, 1H, Ar-H), 7.56 (dd, J = 8.5, 3.6 Hz, 4H, Ar-H), 7.31 (d, J = 8.0 Hz, 2H, Ar-H), 7.01 (d, J = 8.9 Hz, 2H, Ar-H), 4.46 (s, 2H, SCH<sub>2</sub>), 4.07 – 4.01 (m, 2H, OCH<sub>2</sub>), 1.32 (t, J = 6.9 Hz, 3H, CH<sub>3</sub>). <sup>13</sup>C NMR (101 MHz, DMSO-d<sub>6</sub>) δ (ppm) 163.80, 157.59, 157.12, 150.23, 142.14, 135.68, 134.86, 129.57, 129.15, 126.86, 126.69, 125.01, 124.90, 122.23, 115.30, 114.35, 111.75, 63.25, 33.11, 14.48. HR-MS (ESI) calcd for C<sub>24</sub>H<sub>20</sub>F<sub>3</sub>N<sub>3</sub>OS [M+H]<sup>+</sup>: 456.1357, found: 456.1355.

**4.5.18. *N*-(2,4-dimethoxyphenyl)-2-((4-(trifluoromethyl)benzyl)thio)quinazolin-4-amine (9r)**

White solid, 63.8% yield, Mp 132.8-133.4 °C. <sup>1</sup>H NMR (400 MHz, DMSO-d<sub>6</sub>) δ (ppm) 11.38 (s, 1H, NH), 8.71 (d, J = 8.2 Hz, 1H, Ar-H), 7.97 (t, J = 7.7 Hz, 1H, Ar-H), 7.83 (d, J = 8.3 Hz, 1H, Ar-H), 7.68 (t, J = 7.7 Hz, 1H, Ar-H), 7.52 (d, J = 8.1 Hz, 2H, Ar-H), 7.39 (d, J = 8.6 Hz, 1H, Ar-H), 7.15 (d, J = 8.0 Hz, 2H, Ar-H), 6.82 (d, J = 2.4 Hz, 1H, Ar-H), 6.68 (dd, J = 8.6, 2.4 Hz, 1H, Ar-H), 4.32 (s, 2H, SCH<sub>2</sub>), 3.81 (s, 6H, (OCH<sub>3</sub>)<sub>2</sub>). <sup>13</sup>C NMR (101 MHz, DMSO-d<sub>6</sub>) δ (ppm) 164.08, 158.54, 155.22,

142.78, 135.37, 129.48, 128.83, 127.71, 127.39, 126.58, 125.50, 124.90, 124.46, 122.79, 120.28, 118.04, 111.65, 104.73, 99.26, 55.75, 55.49, 33.03. HR-MS (ESI) calcd for  $C_{24}H_{20}F_3N_3O_2S$   $[M+H]^+$ : 472.1307, found: 472.1306.

**4.5.19. *N*-(2,5-dimethoxyphenyl)-2-((4-(trifluoromethyl)benzyl)thio)quinazolin-4-amine (9s)**

White solid, 63.8% yield, Mp 176.0-176.9 °C.  $^1H$  NMR (400 MHz, DMSO- $d_6$ )  $\delta$  (ppm) 9.56 (s, 1H, NH), 8.37 (d,  $J$  = 8.0 Hz, 1H, Ar-H), 7.78 (dd,  $J$  = 11.3, 4.1 Hz, 1H, Ar-H), 7.64 – 7.61 (m, 1H, Ar-H), 7.55 (d,  $J$  = 8.2 Hz, 2H, Ar-H), 7.51 – 7.47 (m, 1H, Ar-H), 7.42 (d,  $J$  = 8.1 Hz, 2H, Ar-H), 7.26 (d,  $J$  = 3.1 Hz, 1H, Ar-H), 7.10 (d,  $J$  = 9.0 Hz, 1H, Ar-H), 6.86 (dd,  $J$  = 9.0, 3.1 Hz, 1H, Ar-H), 4.33 (s, 2H,  $SCH_2$ ), 3.76 (s, 3H,  $OCH_3$ ), 3.73 (s, 3H,  $OCH_3$ ).  $^{13}C$  NMR (101 MHz, DMSO- $d_6$ )  $\delta$  (ppm) 165.40, 157.97, 152.96, 150.13, 147.75, 144.26, 133.40, 129.95, 129.55, 127.47, 126.24, 126.00, 124.93, 124.87, 123.14, 113.21, 112.92, 112.70, 111.36, 56.11, 55.42, 33.24. HR-MS (ESI) calcd for  $C_{24}H_{20}F_3N_3O_2S$   $[M+H]^+$ : 472.1307, found: 472.1307

**4.5.20. *N*-(3,4-dimethoxyphenyl)-2-((4-(trifluoromethyl)benzyl)thio)quinazolin-4-amine (9t)**

White solid, 84.2% yield, Mp 174.1-175.1 °C.  $^1H$  NMR (400 MHz, DMSO- $d_6$ )  $\delta$  (ppm) 11.53 (s, 1H, NH), 8.77 (d,  $J$  = 8.2 Hz, 1H, Ar-H), 7.97 (t,  $J$  = 7.7 Hz, 1H, Ar-H), 7.81 (d,  $J$  = 8.3 Hz, 1H, Ar-H), 7.67 (t,  $J$  = 7.6 Hz, 1H, Ar-H), 7.54 (d,  $J$  = 8.1 Hz, 2H, Ar-H), 7.35 (d,  $J$  = 2.0 Hz, 1H, Ar-H), 7.32 (s, 1H, Ar-H), 7.30 (s, 1H, Ar-H), 7.21 (dd,  $J$  = 8.6, 2.0 Hz, 1H, Ar-H), 7.05 (d,  $J$  = 8.7 Hz, 1H, Ar-H), 4.48 (s, 2H,  $SCH_2$ ), 3.78 (s, 3H,  $OCH_3$ ), 3.75 (s, 3H,  $OCH_3$ ).  $^{13}C$  NMR (101 MHz, DMSO- $d_6$ )  $\delta$  (ppm) 163.90, 157.70, 148.66, 147.63, 142.18, 135.69, 129.59, 127.88, 127.56, 126.84, 125.46, 124.99, 124.85, 122.75, 119.17, 117.57, 111.75, 111.50, 109.91, 55.69, 55.64, 33.14. HR-MS (ESI) calcd for  $C_{24}H_{20}F_3N_3O_2S$   $[M+H]^+$ : 472.1307, found: 472.1304.

**4.5.21. *N*-(3-chloro-4-fluorophenyl)-2-((4-(trifluoromethyl)benzyl)thio)quinazolin-4-amine (9u)**

White solid, 80.0% yield, Mp 146.1-146.4 °C.  $^1H$  NMR (400 MHz, DMSO- $d_6$ )  $\delta$  (ppm) 10.07 (s, 1H, NH), 8.45 (d,  $J$  = 8.2 Hz, 1H, Ar-H), 8.10 (dd,  $J$  = 6.8, 2.6 Hz, 1H, Ar-H), 7.83 (t,  $J$  = 7.6 Hz, 1H, Ar-H), 7.76 – 7.72 (m, 1H, Ar-H), 7.69 (d,  $J$  = 8.0 Hz, 1H, Ar-H), 7.62 (s, 4H, Ar-H), 7.55 (t,  $J$  = 7.3 Hz, 1H, Ar), 7.44 (t,  $J$  = 9.1 Hz, 1H, Ar), 4.49 (s, 2H,  $SCH_2$ ).  $^{13}C$  NMR (101 MHz, DMSO- $d_6$ )  $\delta$  (ppm) 165.07, 157.13, 149.83, 143.64, 135.88, 135.85, 133.77, 129.58, 127.61, 127.29, 126.19, 125.27, 125.05, 124.36, 123.26, 123.03, 118.94, 116.66, 112.94, 33.41. HR-MS (ESI) calcd for  $C_{22}H_{14}ClF_4N_4O_2S$   $[M+H]^+$ : 464.0611, found: 464.0610.

**4.5.22. 2-((4-(Trifluoromethyl)benzyl)thio)-*N*-(3,4,5-trimethoxyphenyl)quinazolin-4-amine (9v)**

White solid, 74.7% yield, Mp 162.6-163.1 °C.  $^1H$  NMR (400 MHz, DMSO- $d_6$ )  $\delta$  (ppm) 10.68 (s, 1H, NH), 8.68 (d,  $J$  = 8.0 Hz, 1H, Ar-H), 7.88 (t,  $J$  = 7.5 Hz, 1H, Ar-H), 7.75 (d,  $J$  = 8.2 Hz, 1H, Ar-H), 7.62 – 7.54 (m, 3H, Ar-H), 7.48 (d,  $J$  = 7.4 Hz, 2H, Ar-H), 7.22 (s, 2H, Ar-H), 4.50 (s, 2H,  $SCH_2$ ), 3.79 (s, 6H,  $(OCH_3)_2$ ), 3.65 (s, 3H,  $OCH_3$ ).  $^{13}C$  NMR (101 MHz, DMSO- $d_6$ )  $\delta$  (ppm) 164.74, 157.39, 152.58,

143.35, 134.88, 134.26, 134.05, 129.68, 127.67, 127.36, 125.66, 125.52, 125.02, 124.17, 122.82, 112.71, 101.71, 60.10, 55.90, 33.28. HR-MS (ESI) calcd for  $C_{25}H_{22}F_3N_3O_3S$   $[M+H]^+$ : 502.1412, found: 502.1413.

## 5. Materials and Methods

### 5.1 Materials

All compounds were dissolved in DMSO to make a 10 $\mu$ M stock solution. RPMI-1640 and MTT were purchased from Solarbio. Fetal Bovine Serum (FBS) was obtained from Tianhang Biotechnology Co. Annexin V-FITC/PI Apoptosis Detection Kit and Cell Cycle Detection Kit were purchased from Keygen Biotech. Dihydroethidium kit was purchased from Beyotime Biotechnology. Bax and p53 polyclonal antibodies were purchased from Proteintech; Bcl-2 monoclonal antibodies and Phospho-EGF Receptor Antibody Sampler Kit were purchased from CST. PI3 Kinase Monoclonal Antibody and PI3 Kinase (phospho-Tyr467/199) Antibody were purchased from SAB. Phospho-AKT (Ser473) rabbit polyclonal antibody and AKT rabbit polyclonal antibody were purchased from SAB. GAPDH rabbit monoclonal antibody was purchased from Good-Here Biotechnology. All the other reagents used were of analytical grade.

### 5.2 Cell culture and treatment

Human cancer cells MDA-MB-231, MCF-7, PC-3, HGC-27 and MGC-803 were purchased from American Type Culture Collection (ATCC, Shanghai, China). All of them were cultured in RPMI-1640 with 10% FBS. Cells were cultured at 37 °C in a humidified atmosphere of 5% CO<sub>2</sub> and were stimulated with different concentrations of 9n. Cells were fed every 2–3 days and sub-cultured when they reached 70–80% confluence.

### 5.3 MTT assay

Cells in the logarithmic growth phase were seeded in 96-well plates at 3,000-5,000 cells per well. After the cells were cultured for 24h, different concentrations of compound 9n were treated for 24, 48 and 72h, respectively. MTT (3-[4,5-dimethylthiazol-2-yl]-2, 5-diphenyltetrazolium bromide, Solarbio) was added to each well at a final concentration of 0.5 mg/ml. After 4h in a 37 °C incubator, the medium was aspirated. 150 $\mu$ l DMSO was then added to each well to dissolve the formazan, and the plate was shaken on a shaker for 10 minutes. The absorbance was measured by an enzyme-linked immunosorbent assay reader (BioTek, USA) at a wavelength of 490 nm, and the cell survival rate was measured. Viability rate = Abs 490 treated cells/Abs 490 control cells  $\times$  100%. The concentration-response curve generated by SPSS 16.0 software was used to determine the concentration of compound (IC<sub>50</sub>) required to inhibit cell growth by 50%. Cell viability curves were

generated using GraphPad Prism 7.0 software at various concentrations of all compounds. Results were Mean  $\pm$  SD of three independent experiments.

#### 5.4 Colony formation assay

MDA-MB-231 and MCF-7 cells in the logarithmic growth phase were plated in a 6-well plate at a density of 500 cells per well, and then the cells were cultured at 37 °C in a 5%CO<sub>2</sub> humidified atmosphere. After the cells were cultured for 24h, different concentrations (0, 3, 6, 9 $\mu$ M) of compound 9n were treated for 7 days. The cells were incubated with ice methanol for 10 minutes and stained with 0.1% crystal violet solution. After the plate is naturally dried, images were photographed. Morphological analysis was performed through microscopy (Leica EZ4W, China). The experiment was repeated three times.

#### 5.5 Cell cycle analysis

MDA-MB-231 and MCF-7 cells in the logarithmic growth phase were plated in a six-well plate at a density of  $2 \times 10^5$  cells per well. After the cells were cultured for 24h, different concentrations (0, 3, 6, 12 $\mu$ M) of compound 9n were administered for 24h. The cells were harvested with trypsin, washed with PBS (phosphate-buffered saline) and incubated in pre-cooled 70% ethanol overnight at 4 °C. The cells were collected and detected by the cell cycle detection kit (Keygen Biotech, China), according to the manufacturer's protocol. Briefly, cells were washed with ice-cold PBS, and resuspended in RNase A solution and propidium iodide (PI) solution. Then the mixture was incubated at room temperature for 30 minutes in the dark. Ten thousand cells were collected and analyzed. Cell cycle progression of each sample was measured by FAC-SCalibur flow cytometer (BD, Biosciences, San Jose, CA, USA) and data was processed using ModFit LT software.

#### 5.6 Scratch assay

MDA-MB-231 and MCF-7 cells in the logarithmic growth phase were collected and seeded in 6-well plates at  $1.5 \times 10^5$  cells per well. After the cells were cultured for 24h, "wound" was drawn at the bottom of the plate. Cells were cultured in RPMI-1640 medium containing 2% FBS. Photos were taken with a microscope as control groups. Different concentrations (0, 2, 4, 6 $\mu$ M) of compound 9n were treated for 72h. Take photos again as experimental groups. Three fields were randomly selected from each sample. Images were processed with Photoshop and Illustrator software.

#### 5.7 Cell morphology analysis and DAPI staining

MDA-MB-231 and MCF-7 cells in the logarithmic growth phase were plated in a 6-well plate at a density of  $2 \times 10^5$  cells per well. After the cells were cultured for 24h, different concentrations (0, 2, 4, 8 $\mu$ M) of compound 9n were treated for 48h. Then, the cells were incubated with pre-cooled methanol at 4 °C for 10 min, and resuspended in the DAPI dye solution in the dark. Three fields of each sample

were selected and photographed with a fluorescence microscope (Nikon Eclipse Ti-S, Nikon Ltd, Japan), and the images were processed with Photoshop and Illustartor software.

### 5.8 Analysis of apoptosis by flow cytometry

MDA-MB-231 and MCF-7 cells in the logarithmic growth phase were plated in a six-well plate at a density of  $2 \times 10^5$  cells per well. After the cells were cultured for 24h, different concentrations (0, 2, 4, 6 $\mu$ M) of compound 9n were treated for 48h. The cells were collected and measured with the Annexin V-FITC/PI Apoptosis Detection Kit (Keygen Biotech, China), according to the manufacturer's protocol. Briefly, cells were washed with ice-cold PBS, and resuspended in Annexin V-FITC solution and propidium iodide (PI) solution. The mixture was incubated at room temperature for 30 minutes in the dark. The FAC-SCalibur flow cytometer (BD Biosciences, San Jose, CA, USA) was used to detect apoptosis in each sample, and data was analyzed using Flow Jo software.

### 5.9 Intracellular ROS assay

MDA-MB-231 and MCF-7 cells in the logarithmic growth phase were plated in a six-well plate at a density of  $2 \times 10^5$  per well. After the cells were cultured for 24h, different concentrations (0, 2, 4, 8 $\mu$ M) of compound 9n were administrated for 48h. Then, the cells were incubated in DHE solution at 37 °C for 30 min in the dark. Three fields were selected for each sample and photographed with a fluorescence microscope (Nikon Eclipse Ti-S, Nikon Ltd, Japan). Process images with Photoshop and Illustartor software

### 5.10 Western blot analysis

Western blot were performed as described in the previous study [32]. The cells were treated with compound 9n at 0, 3, 6 and 12 $\mu$ M. The intracellular proteins were extracted the RIPA lysate buffer (Beyotime Biotechnology) and the protein contents were determined by the BCA protein quantification kit (Beyotime Biotechnology). Total proteins were separated by the SDS-PAGE according to the molecular weight. Blots were blocked at room temperature for 2h in 5% nonfat dry milk-PBS-0.05% Tween 20. The primary antibody (1:1000) was incubated overnight at 4 °C and then washed three times with PBS-Tween20 (0.05%) for 10 min/time. The horseradish peroxidase-conjugated secondary antibody (1:10,000) was incubated for 2h at room temperature and then washed three times with PBS-Tween20 (0.05%) for 10 min/time. Blots exposure was performed with an ECL chemiluminescence solution. All bands were analyzed Image J software. All the above experimental results were repeated three times.

### 5.11 Molecular docking

Molecular docking study was performed using MOE 2014. The protein of EGFR (PDB code:2ITO) and PI3K (PDB code:3APC) was downloaded from RCSB Protein Data Bank. The crystal structure of EGFR and PI3K were selected as acceptor and prepared using default parameters in the QuickPrep module. The protonation states of the ionizable residues were adjusted at pH=7. The 3D structures of all compounds were prepared by taking energy minimization and conformational search. The pose with the best score was used to explain the binding model of compound 9n in the active site of protein.

### 5.12 Statistical analysis

All experimental data are the results of the experiment repeated three times. Statistical analysis operations and mapping were done using Photoshop, ImageJ, SPSS, Graph Pad, etc. All experimental results are expressed as Mean  $\pm$  SD. The mean comparison between groups was performed by ONE-WAY ANOVA and the Turkey method.  $P < 0.05$  was considered statistically significant.

### Acknowledgments

This work was supported by the National Natural Science Foundation of China (No. 81430085), and Natural Science Foundation of Henan (No. 182300410321).

### Conflicts of Interest

There are no conflicts of interest to report.

### References:

- [1] Y. Ji, Q. Sun, J. Zhang, H. Hu, MiR-615 inhibits cell proliferation, migration and invasion by targeting EGFR in human glioblastoma, *Biochem Biophys Res Commun*, 499 (2018) 719-726.
- [2] H. You, K. Meng, Z.Y. Wang, The ER-alpha36/EGFR signaling loop promotes growth of hepatocellular carcinoma cells, *Steroids*, 134 (2018) 78-87.
- [3] M.A. Lemmon, J. Schlessinger, Cell signaling by receptor tyrosine kinases, *Cell*, 141 (2010) 1117-1134.
- [4] X. Qu, L. Yang, Q. Shi, X. Wang, D. Wang, G. Wu, Lidocaine inhibits proliferation and induces apoptosis in colorectal cancer cells by upregulating mir-520a-3p and targeting EGFR, *Pathol Res Pract*, 214 (2018) 1974-1979.
- [5] R.B. David S. Salomon, Fortunato Ciardiello, Nicola Normanno, Epidermal growth factor-related peptides and their receptors in human malignancies, *Critical Reviews in Oncology/Hematology* 19 (1994) 183-232.
- [6] W. Li, Q. Sun, L. Song, C. Gao, F. Liu, Y. Chen, Y. Jiang, Discovery of 1-(3-aryl-4-chlorophenyl)-3-(p-aryl)urea derivatives against breast cancer by inhibiting PI3K/Akt/mTOR and Hedgehog signalings, *Eur J Med Chem*, 141 (2017) 721-733.
- [7] X. Yang, Y. Ding, M. Xiao, X. Liu, J. Ruan, P. Xue, Anti-tumor compound RY10-4 suppresses multidrug resistance in MCF-7/ADR cells by inhibiting PI3K/Akt/NF-kappaB signaling, *Chem Biol Interact*, 278 (2017) 22-31.
- [8] Z. Liu, Q. Zheng, W. Chen, M. Wu, G. Pan, K. Yang, X. Li, S. Man, Y. Teng, P. Yu, W. Gao, Chemosensitizing effect of Paris Saponin I on Camptothecin and 10-hydroxycamptothecin in lung cancer cells via p38 MAPK, ERK, and Akt signaling pathways, *Eur J Med Chem*, 125 (2017) 760-769.

- [9] D.A. Fruman, H. Chiu, B.D. Hopkins, S. Bagrodia, L.C. Cantley, R.T. Abraham, The PI3K Pathway in Human Disease, *Cell*, 170 (2017) 605-635.
- [10] S. Liebscher, L. Koi, S. Lock, M.H. Muders, M. Krause, The HIV protease and PI3K/Akt inhibitor nelfinavir does not improve the curative effect of fractionated irradiation in PC-3 prostate cancer in vitro and in vivo, *Clin Transl Radiat Oncol*, 2 (2017) 7-12.
- [11] D. Hanahan, R.A. Weinberg, Hallmarks of Cancer: The Next Generation, *Cell*, 144 (2011) 646-674.
- [12] K. Okkenhaug, M. Graupera, B. Vanhaesebroeck, Targeting PI3K in Cancer: Impact on Tumor Cells, Their Protective Stroma, Angiogenesis, and Immunotherapy, *Cancer Discov*, 6 (2016) 1090-1105.
- [13] Y. Yarden, G. Pines, The ERBB network: at last, cancer therapy meets systems biology, *Nat Rev Cancer*, 12 (2012) 553-563.
- [14] N. Golob-Schwarzl, S. Krassnig, A.M. Toeglhofer, Y.N. Park, M. Gogg-Kamerer, K. Vierlinger, F. Schroder, H. Rhee, R. Schicho, P. Fickert, J. Haybaeck, New liver cancer biomarkers: PI3K/AKT/mTOR pathway members and eukaryotic translation initiation factors, *Eur J Cancer*, 83 (2017) 56-70.
- [15] C. Mendoza-Martinez, J. Correa-Basurto, R. Nieto-Meneses, A. Marquez-Navarro, R. Aguilar-Suarez, M.D. Montero-Cortes, B. Noguera-Torres, E. Suarez-Contreras, N. Galindo-Sevilla, A. Rojas-Rojas, A. Rodriguez-Lezama, F. Hernandez-Luis, Design, synthesis and biological evaluation of quinazoline derivatives as anti-trypanosomatid and anti-plasmodial agents, *Eur J Med Chem*, 96 (2015) 296-307.
- [16] T.S. Patel, S.F. Vanparia, S.A. Gandhi, U.H. Patel, R.B. Dixit, C.J. Chudasama, B.C. Dixit, Novel stereoselective 2,3-disubstituted quinazoline-4(3H)-one derivatives derived from glycine as a potent antimalarial lead, *New Journal of Chemistry*, 39 (2015) 8638-8649.
- [17] A.M. Alafeefy, A.A. Kadi, O.A. Al-Deeb, K.E. El-Tahir, N.A. Al-Jaber, Synthesis, analgesic and anti-inflammatory evaluation of some novel quinazoline derivatives, *Eur J Med Chem*, 45 (2010) 4947-4952.
- [18] H.M. Patel, M.N. Noolvi, A.A. Shirkhedkar, A.D. Kulkarni, C.V. Pardeshi, S.J. Surana, Anti-convulsant potential of quinazolinones, *RSC Advances*, 6 (2016) 44435-44455.
- [19] S. Lin, Y. Li, Y. Zheng, L. Luo, Q. Sun, Z. Ge, T. Cheng, R. Li, Design, synthesis and biological evaluation of quinazoline-phosphoramidate mustard conjugates as anticancer drugs, *Eur J Med Chem*, 127 (2017) 442-458.
- [20] A. Inoue, K. Kobayashi, K. Usui, M. Maemondo, S. Okinaga, I. Mikami, M. Ando, K. Yamazaki, Y. Saijo, A. Gemma, H. Miyazawa, T. Tanaka, K. Ikebuchi, T. Nukiwa, S. Morita, K. Hagiwara, First-line gefitinib for patients with advanced non-small-cell lung cancer harboring epidermal growth factor receptor mutations without indication for chemotherapy, *J Clin Oncol*, 27 (2009) 1394-1400.
- [21] C.E. Geyer, J. Forster, D. Lindquist, S. Chan, C.C. Romieu, T. Pienkowski, A.J. Gruszfeld, J. Crown, A. Chan, B. Kaufman, D. Skarlos, M. Campone, N. Davidson, M. Berger, C. Oliva, S.D. Rubin, S. Stein, D. Cameron, Lapatinib plus Capecitabine for HER2-Positive Advanced Breast Cancer, *N Engl J Med*, 355 (2006) 2733-2743.
- [22] M.J. Moore, D. Goldstein, J. Hamm, A. Figer, J.R. Hecht, S. Gallinger, H.J. Au, P. Murawa, D. Walde, R.A. Wolff, D. Campos, R. Lim, K. Ding, G. Clark, T.V. Nomikos, M. Ptasynski, W. Parulekar, Erlotinib plus gemcitabine compared with gemcitabine alone in patients with advanced pancreatic cancer: a phase III trial of the National Cancer Institute of Canada Clinical Trials Group, *J Clin Oncol*, 25 (2007) 1960-1966.
- [23] M.H. Cohen, J.R. Johnson, Y.F. Chen, R. Sridhara, R. Pazdur, FDA Drug Approval Summary: Erlotinib (Tarceva®) Tablets, *The Oncologist*, 10 (2005) 416-466.
- [24] M.H. Cohen, G.A. Williams, G.C. Rajeshwari Sridhara, J. W. David McGuinn, D. Morse., S. Abraham, A. Rahman, C. Liang, R. Lostritto, A. Baird, R. Pazdur, United States Food and Drug Administration Drug Approval Summary: Gefitinib(ZD1839; Iressa) Tablets, *Clinical Cancer Research*, 10 (2004) 1212-1218.
- [25] V. Alagarsamy, K. Chitra, G. Saravanan, V.R. Solomon, M.T. Sulthana, B. Narendhar, An overview of quinazolines: Pharmacological significance and recent developments, *Eur J Med Chem*, 151 (2018) 628-685.

- [26] K. Kohda, I. Terashima, K. Koyama, K. Watanabe, K. Minerura, Potentiation of the Cototoxicity of Chloroethylnitrosourea by  $O^6$ -Arylmethylguanines, *Biol Pharm Bull*, 18 (1995) 424-430.
- [27] S. Hanessian, L. Auzzas, G. Giannini, M. Marzi, W. Cabri, M. Barbarino, L. Vesci, C. Pisano, Omega-alkoxy analogues of SAHA (vorinostat) as inhibitors of HDAC: a study of chain-length and stereochemical dependence, *Bioorg Med Chem Lett*, 17 (2007) 6261-6265.
- [28] F. Thuaud, S. Kojima, G. Hirai, K. Oonuma, A. Tsuchiya, T. Uchida, T. Tsuchimoto, M. Sodeoka, RE12 derivatives displaying Vaccinia H1-related phosphatase (VHR) inhibition in the presence of detergent and their anti-proliferative activity against HeLa cells, *Bioorg Med Chem*, 22 (2014) 2771-2782.
- [29] B. Wei, Q. Lin, Y.G. Ji, Y.C. Zhao, L.N. Ding, W.J. Zhou, L.H. Zhang, C.Y. Gao, W. Zhao, Luteolin ameliorates rat myocardial ischaemia-reperfusion injury through activation of peroxiredoxin II, *Br J Pharmacol*, 175 (2018) 3315-3332.
- [30] S. Chou, W.K. Yin, Y.S. Chung, L.S. Chang, C.W. Liu, S.F. Chen, K.S. Shih, Kilogram-Scale Synthesis of a Highly Selective  $\alpha_1$ -Adrenoceptor Antagonist (DL-028A), *Organic Process Research & Development*, 6 (2002) 273-278.
- [31] M.A. Qhobosheane, A. Petzer, J.P. Petzer, L.J. Legoabe, Synthesis and evaluation of 2-substituted 4(3H)-quinazolinone thioether derivatives as monoamine oxidase inhibitors, *Bioorg Med Chem*, 26 (2018) 5531-5537.
- [32] Q. Lin, X.-Y. Chen, J. Zhang, Y.-L. Yuan, W. Zhao, B. Wei, Upregulation of SIRT1 contributes to the cardioprotective effect of Rutin against myocardial ischemia-reperfusion injury in rats, *Journal of Functional Foods*, 46 (2018) 227-236.

**Highlights**

- The 2,4-disubstituted quinazolines showed moderate to good growth inhibition against the tested five human cancer cells.
- Among them, compound **9n** exerted the most excellent anti-proliferative activities against breast cancer cells.
- Compound **9n** inhibited the colony formation and migration of MDA-MB-231 and MCF-7 cells.
- Compound **9n** caused cell cycle arrest at G1 phase and induced apoptosis of MDA-MB-231 and MCF-7 cells.
- Compound **9n** inhibited tumor growth through EGFR-PI3K signaling pathway.